

12

AFGL-TR-84-0066

ANALYSIS AND PROGRAMMING FOR RESEARCH
IN THE PHYSICS OF THE UPPER ATMOSPHERE

JAMES N. BASS
FRANK R. ROBERTS

LOGICON, INC.
18 HARTWELL AVENUE
LEXINGTON, MASSACHUSETTS 02173

FINAL SCIENTIFIC REPORT
1 OCTOBER 1982 - 30 SEPTEMBER 1983

1 FEBRUARY 1984

APPROVED FOR PUBLIC RELEASE; DISTRIBUTION UNLIMITED

AIR FORCE GEOPHYSICS LABORATORY
AIR FORCE SYSTEMS COMMAND
UNITED STATES AIR FORCE
HANSCOM AFB, MASSACHUSETTS 01731

DTIC
ELECTE
AUG 9 1984
B

AD-A144 203

DTIC FILE COPY

84 08 09 053

This report has been reviewed by the ESD Public Affairs Office (PA) and is releasable to the National Technical Information Service (NTIS).

This technical report has been reviewed and is approved for publication

Edward H. Robinson

(Signature)

Name

Contract Manager

Robert E. Manning

(Signature)

Name

Branch Chief

FOR THE COMMANDER

Emmie C. Brown

(Signature)

Name

Division Director

Qualified requestors may obtain additional copies from the Defense Technical Information Center. All others should apply to the National Technical Information Service.

If your address has changed, or if you wish to be removed from the mailing list, or if the addressee is no longer employed by your organization, please notify AFGL/DAA, Hanscom AFB, MA 01731. This will assist us in maintaining a current mailing list.

Do not return copies of this report unless contractual obligations or notices on a specific document requires that it be returned.

UNCLASSIFIED

SECURITY CLASSIFICATION OF THIS PAGE (When Data Entered)

REPORT DOCUMENTATION PAGE		READ INSTRUCTIONS BEFORE COMPLETING FORM
1. REPORT NUMBER AFGL-TR-84-0066	2. GOVT ACCESSION NO. AD-A144203	3. REPORT CATALOG NUMBER
4. TITLE (and Subtitle) Analysis and Programming for Research in the Physics of the Upper Atmosphere	5. TYPE OF REPORT & PERIOD COVERED Scientific - Final 1 Oct 1982 - 30 Sep 1983	
7. AUTHOR(s) James N. Bass Frank R. Roberts	6. PERFORMING ORG. REPORT NUMBER LSIS84156 ESD-001	
9. PERFORMING ORGANIZATION NAME AND ADDRESS Logicon, Inc. 18 Hartwell Avenue Lexington, MA 02173	8. CONTRACT OR GRANT NUMBER(s) F19628-80-C-0175	
11. CONTROLLING OFFICE NAME AND ADDRESS Air Force Geophysics Laboratory Hanscom AFB, MA 01731 Contract Monitor: Edward C. Robinson/RMY	10. PROGRAM ELEMENT, PROJECT, TASK AREA & WORK UNIT NUMBERS 62101F 9993XXXX	
14. MONITORING AGENCY NAME & ADDRESS (if different from Controlling Office)	12. REPORT DATE 1 February 1984	
	13. NUMBER OF PAGES 88 Pages	
	15. SECURITY CLASS. (of this report) Unclassified	
	16a. DECLASSIFICATION/DOWNGRADING SCHEDULE	
16. DISTRIBUTION STATEMENT (of this Report) Approved for Public release; distribution unlimited		
17. DISTRIBUTION STATEMENT (of the abstract entered in Block 20, if different from Report)		
18. SUPPLEMENTARY NOTES		
19. KEY WORDS (Continue on reverse side if necessary and identify by block number)		
Accelerometer Atmospheric Density Model Atmospheric Drag Atmospheric Tides Computer Programs	Doppler Beacon Ephemeris HF Propagation Orbital Dynamics Radio Wave Duct	Satellite Scintillation
20. ABSTRACT (Continue on reverse side if necessary and identify by block number)		
<p>Studies are available in the literature for evaluating local time variations of the density of the atmosphere imparted by tidal effects. Methods are reported here for incorporating the results of these analyses into easily computed formulations of the dependence on local time of the temperature and density. The Jacchia-Bass density model has been</p> <p style="text-align: right;">(Continued)</p>		

Best Available Copy

UNCLASSIFIED

SECURITY CLASSIFICATION OF THIS PAGE(When Data Entered)

cont modified to simplify calculations by excluding from consideration those minor constituents whose total contribution to the mass density is less than 1%.

Software ^{was} ~~has been~~ developed to support studies of atmospheric density variations based on data collected by satellite-borne accelerometers.

Modifications ^{were} ~~have been~~ made to several standard satellite ephemeris codes. The changes include: (1) adaptation of the imbedded atmospheric density model to extend its validity to cases of extremely high solar activity; and (2), improvement in the accuracy of conversion between mean Keplerian elements and position/ velocity vectors.

A spurious signal originating in the receiver is found to contaminate recorded data from scintillating trans-ionospheric radio waves transmitted from a satellite beacon. Special pre-processing is shown to eliminate the effect of the contaminant on statistical analyses of the scintillation data.

An HF ducted mode of propagation is to be supported using artificial ionospheric irregularities. One terminal is to be ground-based; the other, satellite-borne. A standard satellite ephemeris program has been augmented to provide time histories of range and range-rate for both the ducted mode and the classical ionospheric reflection modes.

UNCLASSIFIED

Acknowledgment

The support and guidance of Ms. Eunice C. Cronin, Computer Center Branch Chief, Mr. Robert E. McInerney, Data systems Section Chief, and Mr. Edward C. Robinson, Contract Monitor, are greatly appreciated. Thanks are due also to the various AFGL investigators, with whom we have been associated, whose motivation and direction have consistently benefitted our participation in AFGL research.

Mr. Charles M. O'Berg, of the Logicon technical staff, contributed substantially to the development of software for this project.

**DTIC
ELECTE**
AUG 9 1984
B



Accession For	
NTIS GRA&I	<input checked="checked" type="checkbox"/>
DTIC TAB	<input type="checkbox"/>
Unannounced	<input type="checkbox"/>
Justification	
By	
Distribution/	
Availability Codes	
Dist	Avail and/or Special
A-1	

Table of Contents

1.0	Atmospheric Density Models	3
1.1	Atmospheric Tides	4
1.1.1	Total Density Tides	5
1.1.2	Jacchia-Bass Tidal Model	18
1.2	Updates to Programs CADNIP and BADMEP	21
1.2.1	Mean Elements - Position/Velocity Transformation	21
1.2.2	Input and Output of Position/Velocity.	27
1.2.3	Thermospheric Response to High Solar Activity.	28
1.2.4	Addenda to CADNIP and BADMEP User's Manuals.	28
1.2.4.1	Density Model Preparation	28
1.2.4.2	Solar and Geophysical Data.	28
1.2.4.3	CANDIP Starting Elements Cards.	29
1.2.4.4	CADNIP Change Cards	32
1.2.4.5	CADNIP Run Card	32
1.2.4.6	Description of CADNIP Parameter Table	33
1.2.4.7	Output from CADNIP.	33
1.2.4.8	BADMEP Input.	35
1.3	Neglect of Minor Constituents	36
1.4	Satellite Accelerometer Data Studies.	37
1.4.1	Data Bases for Density Model Evaluation.	38
1.4.2	Statistical Evaluation of Density Models	49
1.4.3	Studies of the Semiannual Variation.	51
1.5	References.	59
2.0	Artifacts in SPA Observations of Radio Wave Scintillations	63
2.1	Introduction.	63
2.2	Contamination of SPA Signals.	63
2.3	Suppression of Leakage.	68
2.4	References.	72
3.0	Program PROPLOK.	73
3.1	Introduction.	73
3.2	Functional Description.	74
3.3	Input and Output.	77
3.4	Mathematical Approach	78
3.4.1	Propagation Geometries	78
3.4.1.1	Classical Modes	78
3.4.1.2	Ducted Mode	82
3.4.2	Propagation Range Rate	82
3.4.2.1	Classical Modes	82
3.4.2.2	Ducted Mode	84
3.5	References	84

List of Figures

<u>Sect.</u>	<u>No.</u>		<u>Page</u>
1.	1	Program TIDEVAR Inputs and Outputs	7,8
	2	Program STAT Sample: Three Dimensional Bins	46
	3	Sample Program STAT Output	52
	4	Software for Studying the Semiannual Variation . . .	54
	5	Sample of Normalized Data for the Semiannual Variation	55
2.	1	Simplified Schematic of SPA Receiver	64
	2	Effect of Coherent Leakage in the Time Domain. . . .	65
	3	Spectrograms Exhibiting Presence of Coherent Leakage.	66
	4	Sketches of Signal Scatter Plots Illustrating Effect of Offset Frequency and Coherent Leakage. . .	70
	5	Illustration of Elimination of Coherent Leakage. . .	71
3.	1	Propagation Geometry	74
	2	Simplified Operational and Data Flow for PROPLOK . .	76
	3	Sample Output From PROPLOK	79
	4	Geometry of a Single Half-Hop.	81
	5	Ducted Path.	81
	6	Geometry for Range Rate Calculation for Classical Modes.	83
	7	Geometry for Range Rate Calculation for the Ducted Mode.	83

List of Tables

<u>Sect.</u>	<u>No.</u>		<u>Page</u>
1.	1	Thermal and Molecular Diffusion Parameters	9
	2	Coefficients for Total Density Semidiurnal Tide in Regions 1 and 2.	15
	3	Format of Mass Storage File "JSDM" for CADNIP and BADMEP.	30,31
	4	Accelerometer Density Data Base.	39,40
	5	Density Models Computed by Program FOURMOD	40
	6	Program FOURMOD Punched Card Input	42
	7	Program FOURMOD Output Data Base	44
	8	DENDB Output Data Base	45
	9	Punch Card Input for Program STAT.	47
	10	Sample Bin Specification for Program STAT.	48
	11	Program BNSORT Input	56
	12	Program BNSORT Output.	56
	13	Program DAILAV Input and Output.	57
	14	Semiannual Variation	58

1.0 Atmospheric Density Models

This section describes recent analysis and programming performed by Logicon, Inc., to develop improved upper atmospheric neutral density models. Knowledge of upper atmospheric neutral densities is an important requirement for the understanding and analysis of many phenomena under study at AFGL. Researchers in many areas desire best estimates of composition and temperatures as inputs to models and data analysis programs. Prominent examples are analyses of auroral, airglow, and ionospheric measurements.

The continuing need for accuracy in satellite tracking and ephemerides prediction also results in the need for improved modeling of thermospheric density variations. Poorly modeled magnetic storm and local time variations continue to limit satellite tracking and prediction accuracy, particularly at lower altitudes. Operational models used in this application must be not only accurate but also efficient. The computation of satellite drag requires only the total mass density, as opposed to the composition. Thus operational models should be formulated to compute the total mass density directly if possible, or to limit the composition to the most significant components.

Extensive research in atmospheric density modeling has continued at AFGL. Theoretical studies of local time variations have been conducted.¹ Section 1.1 describes Logicon's efforts to incorporate the results of these studies into easily computable formulations of temperature and density local time variations. Section 1.2 discusses modifications made to AFGL's CADNIP/BADMEP² system for satellite orbital decay analysis and prediction. Some of these modifications are temporary changes to an existing density model for studies at extremely high solar activity. In addition permanent modifications have been made to correct an inaccuracy in the conversion between mean elements and position-velocity and to permit direct input/output of position-velocity. Section 1.3 describes a modification to the

Jacchia-Bass³ density model to exclude components whose total contribution to the total mass density is less than 1%. Finally, Section 1.4 describes software developed for studies of atmospheric density variations using satellite accelerometer data collected by AFGL scientists^{4,5,6}.

1.1 Atmospheric Tides

While the response of the upper atmosphere to geomagnetic activity and unmodeled density waves continue to be the major sources of error in practical neutral thermospheric models, variations with local time are also poorly represented in most models, particularly at low altitudes. This is because the behavior switches from primarily diurnal (24 hour period) at high altitude to semidiurnal (12 hour period) at low altitude,⁷ while much of the data used to construct the models are at high altitudes. An exception to this is the MSIS model,^{8,9} which, however, is based largely on midlatitude data¹⁰. Furthermore, the MSIS model does not represent well the atmospheric response to geomagnetic activity, since it uses only daily averages of the geomagnetic activity index rather than 3-hour averages.

Work by Forbes and Garrett¹ on atmospheric tides encompasses both theoretical considerations and data, in that certain parameters of the model are calibrated from data. In particular, the semidiurnal tide in the thermosphere is composed of two parts:¹¹ that due to direct (in-situ) excitation by solar radiation and ion-neutral momentum coupling, and that due to upward propagation of modes excited in the mesosphere. The in-situ portion is computed by solving a set linearized equations expressing momentum and energy conservation, continuity, and the perfect gas law. In these equations the input solar energy is determined by requiring the exospheric diurnal tide, which is assumed to be in-situ, to agree with data. Fourier decomposition in local time of the heat source determines the semidiurnal/diurnal excitation ratio, which together with the diurnal excitation determined as indicated, provides the semidiurnal heat

input. The contribution due to the upward propagation of tidal modes from the mesosphere is determined by subtracting the computed in-situ tide from available wind and temperature measurements and fitting the residuals to a linear combination of such modes¹¹.

In Section 1.1.1 will be discussed the development of a computationally practical representation of the total density annually averaged semidiurnal tide based on the Forbes-Garrett model just discussed. This requires first a computation of the tidal variations in composition,¹² the results of which are combined with a suitable background composition model to compute total density tides. The resulting semidiurnal tide is then fit to simple functional representations in height and latitude for incorporation into existing semi-empirical codes. Simulation of diurnal phase and amplitude variations¹³ is also discussed. Efforts to develop a temperature tidal representation for use in composition models such as the MSIS and Jacchia-Bass models are discussed in Section 1.1.2.

1.1.1 Total Density Tides

The development of a total mass density tidal model begins with the computation of compositional tides. The computation was carried out following Forbes' formulation^{1,12} in which the height variation of the tidal perturbation in the log of the number density of the i th constituent is governed by the equations:

$$\frac{\partial^2 R_i}{\partial h^2} + \left(\beta_i + \frac{1}{D_i} \frac{\partial D_i}{\partial h} \right) \frac{\partial R_i}{\partial h} + \frac{n\omega}{jD_i} \\ = \frac{1}{D_i} \left\{ \nabla \cdot \bar{V} + \beta_i W - \gamma_i \beta_i D_i \frac{\partial}{\partial h} \gamma_i D_i + \frac{\partial W}{\partial h} + K N_{\ell} \right\}$$

where

$$R_i = \nabla \ln N_i$$

$$\beta_i = - \frac{(1 + \alpha_i)}{T_0} \left\{ \frac{\partial T_0}{\partial h} - \frac{1}{H_{i0}} - \frac{\phi_{i0}}{D_i N_{i0}} \right\}$$

$$\gamma_i = (1 + \alpha_i) \left\{ \frac{1}{T_0} \frac{\partial T'}{\partial h} - \frac{T'}{T_0^2} \frac{\partial T_0}{\partial h} \right\} - \frac{H'_i}{H_{i0}^2}$$

h = altitude

N_i = number density of i th constituent

α_i = thermal diffusion coefficient of i th constituent

T_0 = time averaged temperature

T' = tidal perturbation in temperature

H_{i0} = time averaged scale height of i th constituent

H'_i = tidal perturbation in scale height of i th constituent

D_i = diffusion coefficient of i th constituent through major gas

ϕ_{i0} = time averaged vertical flux of i th constituent

n = zonal wave number (1 for diurnal tide, 2 for semidiurnal tide)

ω = rotation rate of earth

$\nabla \cdot V$ = divergence of horizontal velocity

W = vertical velocity of major gas

$-KN_\ell$ = loss rate of N_i due to chemical reaction with some constituent N_ℓ

$j = \sqrt{-1}$

Program TIDEVAR (Figure 1) was constructed to carry out these computations. This program computes the tidal perturbations for the constituents O_2 , O , N_2 , N , He , Ar , and H . Atomic nitrogen has been included for possible use in future composition studies, although it

```

C      PROGRAM TIDVAR(INPUT,OUTPUT,TAPE1,TAPE2,TAPE3=520,TAPE4=520)
C      THERMOSPHERIC COMPOSITION TIDAL VARIATION PROGRAM
C      FORBES,U. (JOURN. GEOPHYS. RES.,VOL. 83,NO. A8,
C      PP. 3691-3698,1978)
C      DIFFUSIVE EQUILIBRIUM MAY BE ASSUMED,I. E., EQUATION (3)
C      OF FORBES IS SOLVED WITH  $W_1'-W' = 0$ .
C      IF DIFFUSIVE EQUILIBRIUM IS NOT ASSUMED,
C      EQUATION (8) IS SOLVED, BUT THE CHEMISTRY TERM  $KNJ'$ 
C      IS NEGLECTED.
C
C      INPUTS
C      CARD 1 (LIST-DIRECTED)
C      IOPT - BOUNDARY CONDITION INDICATOR (SEE X AND Y BELOW)
C      H0 - BOTTOM REDUCED HEIGHT(IN SCALE HEIGHTS ABOVE GROUND)
C      HN - TOP REDUCED HEIGHT(SCALE HEIGHTS ABOVE GROUND)
C      DH - REDUCED HEIGHT STEP SIZE(SCALE HEIGHTS)
C      X (COMPLEX), Y
C      FOR IOPT=1  X=BOTTOM FUNCTION VALUE,
C                  Y IGNORED
C      FOR IOPT=2  X=FUNCTION VALUE
C                  AT REDUCED HEIGHT Y
C      THE OTHER BOUNDARY CONDITION,
C      THE FIRST DERIVATIVE AT THE TGP,
C      IS SET AUTOMATICALLY FROM
C      DIFFUSIVE EQUILIBRIUM
C      CARD 2 (LIST-DIRECTED)
C      IYR - YEAR
C      IMO - MONTH
C      IDA - DAY
C      XLAT - LATITUDE (DEG)
C      MUST BE 0,15,30,45,60,75, OR 90
C      IF 90, THEN ALL THE PREVIOUS 6 LATITUDES
C      WILL BE COMPUTED
C      IMOL - MOLECULAR SPECIE
C      1. O2
C      2. O
C      3. N2
C      4. N
C      5. HE
C      6. AR
C      7. H
C      8. ALL OF THE ABOVE
C      IDIFEQ - 0  DIFFUSIVE EQUILIBRIUM NOT ASSUMED
C              NOT 0  DIFFUSIVE EQUILIBRIUM ASSUMED
C      CARD 3, COL 1-4, A FORMAT
C      MMMM - SOLAR ACTIVITY INDICATOR,
C      "GMIN" OR "GMAX"
C      IF NEITHER THEN BOTH MIN AND MAX WILL BE DONE
C      CARD 4, COL 1-4, A FORMAT
C      DDDD - TIDAL ZONAL WAVE NUMBER INDICATOR,
C      "DIUR" OR "SDIU"
C      IF NEITHER THEN BOTH DIUR AND SDIU WILL BE DONE
C      CARD 5, COL 1-5, I5
C      IDUMP1 - IF NOT ZERO,INTERMEDIATE DUMP IS TRIGGERED
C

```

Figure 1. Program TIDEVAR Inputs and Outputs

C TAPE1 - CARD IMAGES
 C CARDS 1-25 - REDUCED HEIGHTS AND GEOMETRIC HEIGHTS FOR SOLAR
 C MINIMUM
 C $XH(N,1), ZH(N,1), N=1,25$ (3X,F5.2,3X,F5.1)
 C XH = REDUCED HEIGHT (NO. OF SCALE HEIGHTS FROM GROUND)
 C ZH = GEOMETRIC HEIGHT (KM)
 C CARDS 26-50 - REDUCED HEIGHTS AND GEOMETRIC HEIGHTS FOR SOLAR
 C MAXIMUM, IN SAME FORMAT AS FOR MINIMUM.
 C THESE ARE FOLLOWED BY FOUR GROUPS OF 151 CARDS EACH
 C GROUP 1. DIURNAL TIDES, SOLAR MINIMUM
 C GROUP 2. DIURNAL TIDES, SOLAR MAXIMUM
 C GROUP 3. SEMIDIURNAL TIDES, SOLAR MINIMUM
 C GROUP 4. SEMIDIURNAL TIDES, SOLAR MAXIMUM
 C IN EACH GROUP THE CARDS ARE FORMATTED AS FOLLOWS
 C FIRST CARD (CURRENTLY UNUSED)
 C $NZONAL, NMODE$ ISEN(I), I=1,70
 C 212,70A1
 C REMAINING 150 CARDS
 C $((U(I,J,K), UH(I,J,K), I=1,4), J=1,6), K=1,25)$
 C $(F6.2, F4.1, F6.2, F4.1, F6.4, F4.1, F6.2, F4.1)$
 C $U(I,J,K)$ = AMPLITUDE OF ITH TIDAL FIELD,
 C AT JTH LATITUDE AND KTH HEIGHT
 C $UH(I,J,K)$ = CORRESPONDING PHASE (HOURS)
 C TIDAL FIELDS
 C 1. EASTWARD WIND VELOCITY (M/SEC)
 C 2. SOUTHWARD WIND VELOCITY (M/SEC)
 C 3. UPWARD WIND VELOCITY (M/SEC)
 C 4. TEMPERATURE (K)
 C LATITUDES (DEGREES)
 C 1. 0
 C 2. 15
 C 3. 30
 C 4. 45
 C 5. 60
 C 6. 75
 C HEIGHTS ARE GIVEN IN THE XH AND ZH ARRAYS
 C TAPE3 - J70 BACKGROUND DENSITIES
 C TWO BINARY RECORDS, THE FIRST FOR SOLAR MINIMUM,
 C THE SECOND FOR SOLAR MAXIMUM
 C $(HBACK(J,I), (BACKGR(J,K,I), K=1,6), RHO(J,I),$
 C $J=1,23)$
 C $HBACK$ - HEIGHT(KM)
 C $BACKGR$ - BACKGROUND NUMBER DENSITIES (LOG BASE 10,
 C MKS)
 C 1. N2
 C 2. O2
 C 3. O
 C 4. A
 C 5. HE
 C 6. H
 C RHO - TOTAL MASS DENSITY (MKS)
 C OUTPUTS
 C FOR EACH SOLAR ACTIVITY LEVEL AND ZONAL WAVE NUMBER REQUESTED,
 C THE TOTAL DENSITY TIDE IS PRINTED OUT AND WRITTEN TO TAPE 4 IN
 C THE BINARY FORMAT
 C $L, (HH(KK), (RAMP(JJ, KK), RPHASE(JJ, KK), JJ=1,6), KK=1, L)$
 C WHERE
 C L = NUMBER OF HEIGHTS
 C HH = GEOMETRIC HEIGHTS (KM)
 C $RAMP(JJ, KK)$ = AMPLITUDE AT HEIGHT $HH(KK)$, LATITUDE $(JJ-1)*15$ DEGREES
 C $RPHASE(JJ, KK)$ = PHASE IN HOURS, AT THAT HEIGHT AND LATITUDE
 C IF IDUMP1 = 1, DETAILED COMPOSITIONAL TIDES ARE ALSO
 C PRINTED OUT

Figure 1 (Cont'd.)

makes a negligible contribution to the total mass density, as does H in the altitude ranges considered ($h_{\max} = 283\text{km}$ for solar minimum, 420km for solar maximum). The computations can be carried out for 6 latitudes 0, 15, 30, 45, 60, and 75 deg., for both minimum and maximum solar activity (corresponding, approximately, to exospheric temperatures 800K and 1400K, respectively), and for both diurnal and semidiurnal tides. Results are combined with appropriate time averaged background distributions to yield total mass density tides which are written to disk for later use.

The diffusion coefficients are computed as¹⁴

$$D_i = \frac{a_i}{N_0} \left(\frac{T_0}{273.15} \right)^{b_i}$$

where

N_0 = total time averaged number density

T_0 = time averaged temperature

and a_i and b_i are constants given in Table 1, along with the thermal diffusion coefficients α_i .

TABLE 1. Thermal and Molecular Diffusion Parameters

Gas	α_i	a_i ($\text{m}^{-1} \cdot \text{s}^{-1}$)	b_i
O_2	0	4.863×10^{20}	.75
O	0	6.986×10^{20}	.75
N_2	0	6.986×10^{20}	.75
N	0	7.5×10^{20}	.75
He	-0.38	1.7×10^{21}	.691
Ar	0	4.487×10^{20}	.870
H	-0.25	3.305×10^{21}	.5

The background atmosphere, defining N_0 and T_0 , is a latitude independent model defined by Hong and Lindzen¹⁵.

Time averaged vertical flux, important only for H and chemical loss, have been neglected, although they can be easily incorporated later, if warranted, for detailed composition studies. In the altitude range of interest, H is a minor specie; and the only important chemical loss process, O^+ to O_2 charge transfer,¹² affects only the diurnal variation of O_2 . Thus neither of these should have an important effect on total mass density semidiurnal tides.

The tidal perturbations T' , V , and W , are those generated by Forbes and Garrett¹⁶ for the diurnal tide and Garrett and Forbes¹¹ for the semidiurnal tide.

The numerical integration is performed with respect to the reduced height variable,

$$x = \int_0^h \frac{dh}{H}$$

where H is the mean molecular scale height according to the background model. With this change of variable the various derivatives in the governing equation for R_i transform as:

$$\frac{\partial}{\partial h} = \frac{\partial}{\partial x} \frac{\partial x}{\partial h} = \frac{1}{H} \frac{\partial}{\partial x}$$

$$\frac{\partial^2}{\partial h^2} = \frac{\partial}{\partial x} \left(\frac{1}{H} \frac{\partial}{\partial x} \right) = -\frac{1}{H^2} \frac{\partial H}{\partial x} \frac{\partial}{\partial x} + \frac{1}{H} \frac{\partial^2}{\partial x^2}$$

In terms of the new variable x , it is feasible to use a uniform numerical integration grid.

The upper boundary conditions at $h = 283\text{km}$ and 421km for minimum and maximum solar activity, respectively, are defined by diffusive equilibrium:

$$\frac{\partial R_i}{\partial h} = -\gamma_i$$

At the lower boundary, 100km , an attempt was made to calibrate the value of R_i using satellite-borne mass spectrometer data at $140-160\text{km}$ ^{17,18}. This feature is implemented as "Option 2" in the code, in contrast to the normal "Option 1" defined by preset values of R_i at 100km , and the diffusive equilibrium condition, given above, at the upper boundary. This effort proved fruitless, however, as the solutions at $140-160\text{km}$ were quite insensitive to the assumed boundary condition. This is evidently due to the smallness, at 100km , of molecular diffusion, which is the only process, in the model being used, by which molecules at 100km can move vertically upward to affect distributions at higher altitudes. It is possible that the inclusion of eddy diffusion in the model could change this situation. However, based on Reference 14, eddy diffusivities exceed molecular diffusivities by at most a factor of 2 above 100 km for the most important constituents. Therefore the attempt to calibrate the lower boundary condition was dropped, and the fixed condition

$$R_i = 0$$

was adopted.

The numerical integration method employed is that described by Lindzen and Kuo¹⁹ (for one uncoupled differential equation) and Richtmeyer²⁰.

The Jacchia 1970²¹ density model has been used to specify the background composition, since this has been recommended as the best model for satellite use²². The more recent Jacchia-Bass and MSIS models are more expensive computationally than the Jacchia 1970 model while yielding no significant improvements in accuracy²³. The Jacchia 1971²⁴ model, similar to the 1970 model in expense and total density accuracy, represents composition less accurately than the Jacchia 1970 model²².

The resulting semidiurnal tide was fit to the following representations:

Region 1: 120km - 145km

$$\Delta I_{nd} = X(h, \theta) \cos 2at + Y(h, \theta) \sin 2at$$

where

d = total mass density
h = altitude (km)
 θ = latitude
a = earth's rotation rate
t = local time

$$X = \cos^2 \theta \sum_{i=0}^2 \sum_{j=0}^2 \{ A(i,j) + B(i,j) (TINF - 800) \} \cdot (h-145)^i \sin^{2j} \theta$$

$$Y = \cos^2 \theta \sum_{i=0}^2 \sum_{j=0}^2 \{ C(i,j) + D(i,j) (TINF - 800) \} \cdot (h-145)^i \sin^{2j} \theta$$

TINF = global mean, geomagnetically quiet, exospheric temperature (K)

A(i,j), B(i,j), C(i,j), and D(i,j) = adjustable parameters

Region 2: $155\text{km} - h_m$; $h_m = 283\text{km} + 0.23 (\text{TINF}-800)$

Same as Region 1 except:

$$X = \cos^2 \theta \sum_{i=0}^3 \sum_{j=0}^2 \{E(i,j) + F(i,j) (\text{TINF}-800)\} \cdot (h-155)^i \sin^{2j} \theta$$

$$Y = \cos^2 \theta \sum_{i=0}^3 \sum_{j=0}^2 \{G(i,j) + H(i,j) (\text{TINF} - 800)\} \cdot (h-155)^i \sin^{2j} \theta$$

Region 3: $145\text{km} - 155\text{km}$

Cubic polynomial which matches Region 1 function and slope at 145km and Region 2 function and slope at 155km .

Region 4: h greater than h_m

$$\Delta \ln d = F \Delta_1 \ln d + (1-F) \Delta_2 \ln d$$

where

$$F = M_O n_O \exp \{-b_O(h-h_m)\} / M_T$$

$$M_T = M_O n_O \exp \{-b_O(h-h_m)\} + M_{He} n_{He} \exp \{-b_{He}(h-h_m)\}$$

$$M_O = 16; M_{He} = 4$$

$$\log n_O (/cm^3) = 8.72 - 0.00063 (\text{TINF}-800)$$

$$\log n_{He} (/cm^3) = 6.84 - 0.0003 (\text{TINF}-800)$$

$$b_i = M_i g / (R \cdot \text{TINF})$$

$$g = 9.8 \text{ m/sec}^2$$

$$R = 8314.32 \text{ J(Kg-Mol)}^{-1}/\text{K}$$

$$\Delta_1 \ln d = \Delta \ln d(h_m) + (h - h_m) \frac{\partial \Delta \ln d(h_m)}{\partial h},$$

$$\Delta_2 \ln d = \ln d_0(h, \text{TINF} + \Delta \text{TINF}) - \ln d_0(h, \text{TINF})$$

d_0 = daily average static diffusion density, from tables

$$\Delta \text{TINF} = \cos^2 \theta (c + b \sin^2 \theta)$$

$$c = \cos 2at \{6.4 + 0.086 (\text{TINF} - 800)\} + \sin 2at \{61.15 + 0.0175 (\text{TINF} - 800)\}$$

$$b = \cos 2at \{97.3 - 0.221 (\text{TINF} - 800)\} + \sin 2at \{-156.8 + 0.23 (\text{TINF} - 800)\}$$

Table 2 contains the coefficients for regions 1 and 2. It was found possible to fit these two regions separately to low order polynomials. Fitting the combined region above 120km proved difficult even with 10th order polynomials. Furthermore a piecewise low order fit, as presented here, is preferable to a single high order fit for practical use. The latitudinal dependence hopefully simulates the first 2 or 3 semidiurnal tidal modes and reflects a north-south symmetry. Inclusion of seasonal-latitudinal effects would require terms with odd powers in $\sin \theta$ and functional dependence on the day of the year.

The temperature dependence reflects the assumption of linear behavior between the two limiting cases of minimum solar activity ($\text{TINF} = 800\text{K}$) and maximum solar activity ($\text{TINF} = 1400\text{K}$). The fits obtained in Regions 1 and 2 were quite good for both minimum and maximum solar activity with residuals in $\Delta \ln d$ generally less than 0.03.

High-latitude data, above 45 degrees, was excluded from the fits. An IBM polynomial regression program²⁵ was adapted for use on this effort.

Table 2. Coefficients for Total Density Semidiurnal Tide in Regions 1 and 2

I	J	A	B	C	D
0	0	.13044E+00	-.27508E-05	.10068E-01	-.63314E-04
0	1	-.16696E+01	.69263E-03	-.92293E+00	.74355E-03
0	2	.21901E+01	-.10519E-02	.14035E+01	-.12385E-02
1	0	-.31444E-03	-.77334E-05	-.11168E-01	.16568E-05
1	1	-.11326E-01	.67840E-04	.14079E+00	-.45035E-04
1	2	.14062E-01	-.96105E-04	-.21773E+00	.73289E-04
2	0	-.54921E-03	-.71597E-07	-.24298E-03	.36282E-06
2	1	.77241E-02	-.56474E-06	.46824E-02	-.46413E-05
2	2	-.11647E-01	.12941E-05	-.80633E-02	.75169E-05

I	J	E	F	G	H
0	0	.83092E-01	-.14771E-04	-.66382E-01	-.60025E-05
0	1	-.11248E+01	.54266E-03	.16755E+00	-.15908E-03
0	2	.13615E+01	-.73518E-03	-.14660E+00	.12646E-03
1	0	-.40616E-02	.18762E-05	-.29799E-02	.45295E-05
1	1	.48154E-01	-.40169E-04	.43078E-01	-.57844E-04
1	2	-.69207E-01	.66867E-04	-.50812E-01	.70252E-04
2	0	.38766E-04	-.27673E-07	.78944E-04	-.11124E-06
2	1	-.42412E-03	.42410E-06	-.93818E-03	.13862E-05
2	2	.73694E-03	-.84842E-06	.12074E-02	-.18196E-05
3	0	-.11222E-06	.11483E-09	-.35883E-06	.54577E-09
3	1	.11396E-05	-.14137E-08	.43316E-05	-.67510E-08
3	2	-.23474E-05	.31091E-08	-.57924E-05	.91193E-08

The Region 4 formulation is an attempt to extend the computations above the upper limit, h_m , at which the wind and temperature tides have reached their asymptotic values. Above this point the density tide might be expected to grow linearly in height, controlled by diffusive equilibrium. However, this condition does not occur because there is a change in composition from predominantly atomic oxygen at h_m to helium, and at still higher heights, to hydrogen. In the exospheric limit the simple solution, in which the density is controlled by the temperature, has been adopted. The semidiurnal variation in the exospheric temperature was obtained by 2-point fits to the Garrett-Forbes¹¹ results at 0 and 45 degrees.

The following modifications are suggested to the Jacchia 1970 diurnal tidal model. These are based both on theory¹⁶ and data.^{10,13}

$$T_1 = T_c (1 + R \sin^m x) \left\{ 1 + R \frac{\cos^m x - \sin^m y}{1 + R \sin^m x} \{ b \cos a(t-t_0) + C \} \right\}$$

where

T_1 = geomagnetically quiet exospheric temperature

T_c = global minimum exospheric temperature in original model

$$x = \frac{1}{2} (\theta + d); y = \frac{1}{2} (\theta - d)$$

θ = latitude; d = declination of sun

$$R = 0.31; m = 2.5$$

$$b = 0.35 + 0.00055 (TINF-800)$$

$$c = 0.425$$

TINF = global mean geomagnetically quiet exospheric temperature

$$t_0(\text{hr}) = 14.5 + 6(2.5 \sin^2 2\theta - 1) \exp\{-0.01(h-150)^2\}$$

By comparison the original Jacchia 1970 formulation is:

$$T_1 = T_c (1 + R \sin^m x) \left(1 + R \frac{\cos^m x - \sin^m y}{1 + R \sin^m x} \cos^n \frac{t_a}{2} \right)$$

where

$$n = 3.0$$

$$t_a = \text{function of local time}$$

Thus the only changes are in the local time dependent term, the second term inside the second pair of parentheses. The local time term in the original model is replaced by a purely diurnal term plus a constant which equals the average of the original local time term. The diurnal amplitude factor b is selected to simulate recent data¹⁰ and theory.¹⁶ In particular, measured diurnal density variations at low solar activity indicate that the Jacchia 1971 model diurnal tide, which is nearly the same as in the Jacchia 1970 model, is too high. The temperature amplitude predicted by the Jacchia 1970 model is also higher at low solar activity than that predicted theoretically,¹⁶ while there is closer agreement at high solar activity. The phase depends on the height at which the density is being computed. This phase variation also reflects both data and theory at low altitude.

Eventually, as resources and time permit, an improved representation of the diurnal density tide should be constructed, as was done above for the semidiurnal tide, basing the model directly on density, rather than temperature, variations. The diurnal representation presented here should nevertheless be an improvement over that given in the Jacchia 1970 model, and would be most inaccurate at low altitudes, where the semidiurnal tide dominates.

1.1.2 Jacchia-Bass Tidal Model

In this subsection we discuss the development of an improved tidal model for the Jacchia-Bass density model³. The Jacchia-Bass (JB) model is an adaptation of the Jacchia 1977 model,²⁶ incorporating an analytically integrable temperature profile for the static diffusion equation above 125 km. This feature significantly reduces the computer memory requirements for the solutions to the static diffusion equation (which in the original model must be tabulated numerically for each of 7 components) and thus significantly broadens the range of computers on which the model can be run.

The tidal representation in the Jacchia 1977 model, and hence also in the JB model, is significantly deficient in the semidiurnal tide at low altitudes, as indicated in the previous subsection. In an attempt to capture some detail in the diurnal tides not accommodated in previous models, a height-dependent exospheric temperature diurnal phase is used in the computation of the number density of each constituent.

The model presented here includes a model of the temperature diurnal and semidiurnal tides above 125 km which retains the analytic integrability of the JB model. Analytic expressions for the component number density tides are then immediately obtained, with the exception of boundary conditions and corrections for the effects of winds. Winds should be important above 125 km only for atomic oxygen and minor constituents. In the upper thermospheric region where static diffusion is valid (wind effects negligible), boundary conditions can be obtained from the solutions to the equations governing the composition tidal perturbation discussed in the previous subsection. Departure from static diffusion at lower altitudes can then be obtained by comparison of the exact and static diffusion solutions.

Below 125 km, where departures from static diffusion are large, it is recommended that direct fit to the exact Forbes composition tides be employed.

The temperature model that has been developed above 125 km is as follows:

$$\Delta\left(\frac{1}{T}\right) = \sum_{m=1}^2 (A_m \cos m\omega t + B_m \sin m\omega t)$$

where

T = temperature

ω = rotation rate of earth

t = local time

$$A_m = a_m - e^{-c_m x} \sum_{i=0}^n d_{mi} x^i$$

$$B_m = b_m - e^{-c_m x} \sum_{i=0}^n f_{mi} x^i$$

x = geopotential height above 125 km

$a_m, c_m, d_{mi}, b_m, f_{mi}$ are functions of solar activity and latitude.

The equinox temperature tides computed by Forbes and Garrett (see previous subsection) have been used to determine the parameters $a_m, b_m, c_m, d_{mi}, f_{mi}$ at the latitudes 0, 15, 30, 45, 60, and 75 degrees and for minimum and maximum solar activity ($F_{10.7} = 75$ and 260, respectively, where $F_{10.7}$ is the 10.7 cm solar flux in 10^{-22} watts/m²/Hz).

Least squares multiple regression program STEPR²⁵ was adapted for this purpose. In this program Laguerre polynomials²⁷ were used in place of powers of the geopotential height. This was done in the interest of any efficiency that might be gained in the fitting process from the use of orthogonal functions. A post-processing program LAGTPOW converts the expansions in Laguerre polynomials to power series. An iterative procedure was added to find the optimum parameter c_m , for each latitude and solar activity level. For fixed value of c_m a regression is performed to determine the other parameters. Then a one dimensional search over c_m is made to find the value for which the sum of the squared residuals minimizes. Satisfactory fits were obtained by truncating the power series in the geopotential height x at $n=1$.

The parameters a_m , b_m , d_{mi} , and f_{mi} are next fit as functions of latitude to expansions in the associated Legendre functions P . Only even n is used since symmetry about the equator is assumed. The nonlinear parameters c_m are fit to expansions in Legendre polynomials, again including only the even n functions. Program LATFIT was constructed from program STEPR to perform these latitudinal functional determinations.

Given the temperature profiles above it is possible to obtain immediately the expressions for the tidal perturbations in the number densities under the static diffusion approximation:

$$\Delta \ln N_K = G_K + (1 + \alpha_K) \Delta \ln \left\{ \frac{T(h_0)}{T(h)} \right\} - M_K \Delta F(h)$$

where

N_K = number density of constituent K

h = altitude

$G_K = \Delta \ln N_K(h_0)$

h_0 = reference altitude

α_K = thermal diffusion coefficient of constituent K

T = temperature

M_K = molecular weight of constituent K

$$\Delta F(h) = \frac{g_e R_e^2}{R^* (R_e + 125)^2} \int_{h_0}^h \frac{x(h)}{x(h_0)} \Delta \left(\frac{1}{T} \right) dx$$

g_e = acceleration of gravity

R_e = 6356.766 Km

R^* = universal gas constant

1.2 Updates to Programs CADNIP and BADMEP

Programs CADNIP and BADMEP² have long been used by AFGL scientists in atmospheric density modeling. Program CADNIP is used for density determination by finding, in a least squares sense, the scale factor which, when multiplied by a chosen density model, yields by numerical integration the resulting satellite ephemeris which best fits available tracking data. BADMEP evaluates models by comparing ephemerides generated with them to available tracking data. This section will discuss the following updates:

- o Improvement of routines for converting between mean elements and position/velocity vectors
- o Addition of options to input and output position/velocity directly
- o Temporary modifications to test variants of an existing density model

Discussion of these will be followed by addenda to the CADNIP and BADMEP User's Guides (Appendices A and B of Reference 2) bringing the user fully up to date on usage of the two programs.

1.2.1 Mean Elements - Position/Velocity Transformation

Until recently CADNIP and BADMEP have required input of mean Keplerian elements at some specified time to initiate processing. In CADNIP they are used to develop an initial estimate of the ephemeris for the iterative least squares analysis. In BADMEP they are used to initiate the ephemeris generation for evaluation of the density models. In either case the elements must first be transformed to a position/velocity vector since the numerical integration is done in cartesian coordinates. In addition CADNIP also outputs the mean elements at epoch for the best fit orbit, which requires the reverse transformation: from position/velocity to mean elements.

The transformation from mean elements to position/velocity requires the following two steps:

- 1) Add to the elements the short periodic corrections due to the second harmonic J_2 of the geopotential
- 2) Transform the resulting osculating elements to position/velocity

For the inverse transformation the steps are done in reverse: the osculating elements are formed from the position/velocity vector, and from these the short periodic corrections are subtracted. Note that this definition of the transformation implies that the mean elements are "mean" only with respect to the short-periodic perturbations. This may differ from the "mean" elements supplied by some outside agencies such as ADCOM, whose "mean" elements also exclude long-periodic perturbations due to the third harmonic J_3 . Such elements should be used with care. However in the most common use of such element sets in the CADNIP/BADMEP system, as initial estimates to be refined by CADNIP, extreme accuracy is not a necessity.

A large source of error arises in the computation of the short-periodic corrections to the elements for nearly circular orbits, due to a singularity caused by loss of perigee definition. This has resulted in such anomalies as "negative" eccentricities appearing in the printouts. Aksnes²⁸ has developed a formulation in which the perturbations are computed for a set of intermediate coordinates, the Hill variables:

- r = radius vector
- \dot{r} = time derivative of r
- $G = ka(1-e^2)$
- $H = G \cos i$
- $u = g + f$
- h = right ascension of ascending node

where

k = earth's gravitational constant
a = semimajor axis
e = eccentricity
i = inclination
g = argument of perigee
f = true anomaly

The Hill variables remain well defined for circular orbits and thus the perturbations remain non-singular.

To enable the treatment of nearly circular orbits, the subroutines in CADNIP and BADMEP performing this transformation have been replaced with the following routines.

OSCTMN: main subroutine to convert position and velocity to mean elements
MNTOSC: main subroutine to convert mean elements to position and velocity
PVTHIL: converts position and velocity to Hill variables
HILTMN: converts Hill variables to mean elements
ECCF: computes true anomaly f, ecosf, esinf, and mean anomaly M, given r, \dot{r} and G
MNTHIL: converts mean elements to Hill variables
SHP: computes short-periodic corrections to Hill variables
HILTPV: converts Hill variables to position and velocity

In the computation of the Hill coordinates from position/velocity we have

$$r = \sqrt{x^2 + y^2 + z^2}$$

$$\dot{r} = (x\dot{x} + y\dot{y} + z\dot{z})/r$$

$$G_x = \sqrt{K} (y\dot{z} - z\dot{y})$$

$$G_y = \sqrt{K} (z\dot{x} - x\dot{z})$$

$$G_z = \sqrt{K} (x\dot{y} - y\dot{x})$$

$$G = \sqrt{G_x^2 + G_y^2 + G_z^2}$$

$$H = G_z$$

$$\sqrt{G_x^2 + G_y^2} \sin h = G_x$$

$$\sqrt{G_x^2 + G_y^2} \cos h = -G_y$$

$$\sqrt{x^2 + y^2} \cos \phi = x$$

$$\sqrt{x^2 + y^2} \sin \phi = y$$

$$\sin u = G \sin (\phi - h) \cos \theta / H$$

$$\cos u = \cos (\phi - h) \cos \theta$$

where

$$\theta = \text{latitude}$$

Note that in calculating u , the $\cos \theta$ factor cancels out ($\sin u / \cos u$), and thus need not be calculated. Exceptions are easily handled for equatorial and polar orbits. In the case of equatorial orbits, h is arbitrary, and therefore set to 0, with

$$u = \phi$$

For polar orbits we have

$$\sin u = z/r$$

$$\cos u = \text{SGN}(\dot{z}) \sqrt{1 - \sin^2 u}$$

where $\text{SGN}(X)$ is the algebraic sign of X .

To compute the mean elements from the Hill variables, we compute

$$e \sin f = \dot{r}G/k$$

$$e \cos f = G^2/(kr) - 1$$

$$\frac{r}{a} = \frac{1-e^2}{1+e \cos f}$$

$$e \sin E = \frac{r e \sin f}{a \sqrt{1-e^2}}$$

$$e \cos E = 1 - \frac{r}{a}$$

$$M = E - e \sin E$$

$$g = u - f$$

$$i = \cos^{-1} (H/G)$$

$$a = \{G^2/(1-e^2)\} / k$$

To compute the Hill variables from the mean elements, first the eccentric anomaly is E obtained by solving Kepler's equation

$$M = E - e \sin E$$

Then we have

$$r = a(1 - e \cos E)$$

$$\cos f = (\cos E - e)/(1 - e \cos E)$$

$$\sin f = (\sqrt{1-e^2} \sin E)/(1 - e \cos E)$$

$$u = f + g$$

$$G = \sqrt{ka(1-e^2)}$$

$$H = G \cos i$$

$$\dot{r} = k e \sin f / G$$

To compute the position and velocity from the Hill variables requires

$$x_m = -\frac{H}{G} \sinh$$

$$y_m = \frac{H}{G} \cosh$$

$$z_m = \sqrt{1 - \frac{H^2}{G^2}}$$

$$x_n = \cosh$$

$$y_n = \sinh$$

$$z_n = 0$$

$$\dot{s} = G/r$$

$$x = r (x_m \sin u + x_n \cos u)$$

$$y = r (y_m \sin u + y_n \cos u)$$

$$z = r (z_m \sin u + z_n \cos u)$$

$$\dot{x} = \dot{r}x/r + \dot{s}(x_m \cos u - x_n \sin u)$$

$$\dot{y} = \dot{r}y/r + \dot{s}(y_m \cos u - y_n \sin u)$$

$$\dot{z} = \dot{r}z/r + \dot{s}(z_m \cos u - z_n \sin u)$$

The computation of the short-periodic corrections to the Hill variables is done in accordance with Reference 28, including only terms due to the second harmonic J_2 .

A significant portion of the internal computations of CADNIP and BADMEP is performed in a system of canonical units of length and time, specified by:

- o unit of length = earth radius
- o unit of time = time required for a satellite in an earth radius circular orbit to travel 1 radian.

In these units the earth's gravitational constant k is unity and thus will not appear in equations expressed in these units. Thus one will notice the absence of k on examining much of the CADNIP/BADMEP code, including that just discussed.

1.2.2 Input and Output of Position/Velocity

Options have been added to CADNIP and BADMEP to input position and velocity instead of elements and to output either or both. In the case of CADNIP the user indicates by an input flag whether the starting estimate of the satellite ephemeris is a position/velocity vector or an element set. At the end of each iteration in the differential correction procedure, if such printout is desired, and at the end of the final iteration, CADNIP will print the position/velocity, and/or the element set, at the epoch of the fit span, in accordance with a second input flag. The units in the printouts are km and km/sec, and deg. Punched cards, in NAMELIST format appropriate for BADMEP, are produced, if requested, for the final values of both elements and position/velocity at the epoch of the fit span. For an element set the NAMELIST name is NEWIN, as previously, but for a position/velocity vector the NAMELIST name is NEWINX. The punched position/velocity vector is in canonical units (see end of Section 1.2.1).

BADMEP will read its run parameters from the NAMELIST group NEWIN or the group NEWINX according to an input flag specified on the preceding device control card.

The two groups differ only in that NEWIN includes an element set, while NEWINX includes a position/velocity vector. The cards punched by CADNIP include the time of the elements or vector and the model density factor, as well as the element set or vector. Other inputs must be inserted by the user.

Details of the operation of these options and other features are described in Section 1.2.4.

1.2.3 Thermospheric Response to High Solar Activity

AFGL scientists conducted orbital drag studies over a period of extremely high solar activity, 4-16 November, 1979, with the objective of determining a suitable modification to existing empirical models for such high activity. The Jacchia 1970²¹ model was chosen for this study. Several modifications of the formula for the global nighttime minimum exospheric temperature at zero geomagnetic activity were developed by AFGL researchers. These modifications were implemented in software and made available to AFGL scientists for use in these studies. The modifications were confined to subroutine APFTMP which tabulates solar flux and geomagnetic activity dependent quantities as functions of time. Details of these studies are given elsewhere.²⁹

1.2.4 Addenda to CADNIP and BADMEP User's Manuals

The following are addenda to the CADNIP and BADMEP User's Manuals which are provided in Appendices A and B of Reference 2.

1.2.4.1 Density Model Preparation

The Jacchia 1977 model requires a special mass storage file "JSDM" whose format is given in Table 3.

1.2.4.2 Solar and Geophysical Data

The format of the solar and geophysical file is still as described in Section A.4, Reference 2. However the data must begin at least 2 days

prior to the start of the period to be processed (3 days if the Jacchia 1977 model is used), and there must be a minimum of 308 days of data (462 if the Jacchia 1977 model is used).

1.2.4.3 CADNIP Starting Elements Cards

As indicated in Section 1.2.2, either starting elements or starting position and velocity may be supplied. The user must indicate which by an input option flag in columns 73-75 of the first card of this 2- card set. The value of this flag must be 1 for position and velocity, any other value for elements. An output option flag, in columns 76-78 of the first card, indicates whether elements, position and velocity, or both, at the epoch of the fit span, are to be printed out in the results of the differential correction procedure.

Flag Value	Printout Includes
0	elements only
1	position and velocity only
any other value	both

The remaining parameters of the first card are given as on page 25, Reference 2, except substitute "position and velocity" for "elements" if appropriate.

If position and velocity are to be input, they must appear on the second card as follows:

Columns	Description
1-10	x position (km)
11-20	y position (km)
21-30	z position (km)
31-40	x velocity (km/sec)
41-50	y velocity (km/sec)
51-60	z velocity (km/sec)

In this case the card is read with the format (3F10.4, 3F10.5).

Table 3. Format of Mass Storage File "JSDM"
for CADNIP and BADMEP

Record Number 1		
Word	Symbol	Description
1	LABEL	BCD label
2-9	TITLE	80 Character BCD
10	TMINMOD	Minimum exospheric temp. in table
11	TMAXMOD	Maximum exospheric temp.
12	NTSTEP	Number of Temperature steps
13	DTMOD	Temperature step size
14	NREG (≤ 7)	Number of height regions (=number of subsequent records)
15	NSUM	Unused
16-23	ALZSTEP _i	Natural logs of boundaries (km) of height regions.
24-30	NZSTEP _i	Number of height steps in each region
31-37	ALDZ _i	Step size in natural log of height in each region.
38	GNMOD	Gravitational acceleration at Earth surface (km/sec ²)
39	RNMOD	Earth radius (km)
40	RSTAMOD	Universal gas constant
41	AVOGMOD	Avoquadro's number
42	NSPMOD (6)	Number of species
43-48	AMWMOD _i	Molecular masses of species
49-55	MODRLN _i	Lengths of subsequent records
	$[=(NSPMOD+1) \\ *(NTSTEP+1) \\ *(NZSTEP_i+1)]$	

The species will be given in the order:

O₂, O, N₂, HE AR, H

Table 3 (Cont'd.)

<u>Record Number</u>	<u>IREG+1</u>	<u>1<IREG<NREG)</u>
Word	Description	
1	Local temperature at height exp [ALZSTEP(IREG)] and exospheric temperature TMINMOD	
2 thru NSPMOD+1	Logs base 10 of number densities (m^{-3}) for molecular species at this height and exospheric temperature.	
NSPMOD+2 thru (NTSTEP+1)* (NSPMOD+1)	Repeat of words 1 thru NSPMOD+1 for this height and equally spaced exospheric temperatures TMINMOD + DTMOD thru TMAXMOD	
(NTSTEP+1)*('NSPMOD+1)+1 thru MODRLEN (IREG)	Repeat of words 1 thru (NTSTEP+1)*(NSPMOD+1) for remaining heights exp [ALZSTEP (IREG)] + I *ALDZ (IREG)] I = 1 thru NZSTEP (IREG)	

1.2.4.4 CADNIP Change Cards

The number of the parameter to be changed (field 2, page 26, Reference 2) should appear in columns 16-19. The increase in the field size to 4 columns accommodates the increase in the number of parameters (Section 1.2.4.6).

1.2.4.5 CADNIP Run Card

The currently available density models and the indicators (field 12) are:

- 1 - Jacchia 1964
- 2 - 1966 Supplements
- 3 - Jacchia 1971
- 4 - USSR Cosmos³⁰
- 5 - Jacchia-Walker-Bruce
- 6 - Jacchia 1977²⁶
- 7 - Lockheed/NASA
- 8 - MSIS 77^{8,9}
- 9 - 1962 U.S. Standard
- 10 - MSIS 78³¹
- 11 - DENSEL
- 12 - Jacchia 1970
- 13 - Jacchia 1973
- 14 - Forbes-Garrett-Gillette Model B³²

All the models except 4, 6, 8, 9, 10, 11, and 14 require density tables as described in Section A.3, Reference 2. Model 6 requires the mass storage file JSDB, as described in Section 1.2.4.1 of this report. All the models except 9 and 11 require solar and geomagnetic activity indices as described in Section A.4, Reference 2. Those models without footnotes in the above list are described in Reference 2, Appendix C.

1.2.4.6 Description of CADNIP Parameter Table

The number of parameters has been increased to 1165 to accommodate a gravity model with maximum $m, n = 32$ (previous maximum was 20). The gravity model coefficients are arranged as:

C_{nm} : Parameter number $80 + n(n + 1)/2 + m - 2$

S_{nm} : Parameter number $638 + n(n - 1)/2 + m - 1$

Parameter number 13, if not zero, suppresses printout of the gravity model coefficients, parameters 81 - 1165. The default value of this parameter is 0.

If parameter number 49 is greater than zero, only the preliminary adjustment procedure is run, the differential correction procedure is skipped, and a disk file, TAPE10, is written of all the tracking observations not rejected during the preliminary adjustment procedure. This file is useful for subsequent runs of BADMEP, which does not filter out bad observations. The default value of this parameter is 0.

If parameter number 53 is greater than zero, the final values of the elements and position/velocity at the fit span epoch will be punched out in the NAMELIST format, group name NEWIN and NEWINX, respectively, compatible with input required by BADMEP. The default value of this parameter is 1.

1.2.4.7 Output from CADNIP

All specification cards except the change cards are listed in the printout. This is followed by a printout of the non-zero values of the parameter table, except that parameters 81-1165 are omitted if parameter number 13 is not zero. This is followed by the results of the preliminary adjustment procedure, and the differential correction

procedure. The latter includes position and velocity if requested in accordance with Section 1.2.4.3. The elements and position/velocity are punched in NAMELIST format, as described in Section 1.2.2, if parameter 53 is greater than zero.

In addition, for every successful differential orbit correction a punched card is generated, for post-processing, containing the following information:

<u>Columns</u>	<u>Data</u>	<u>Format</u>	<u>Form</u>
1-3	Day No. of the Year	I3	XXX
4-5	Hour	I2	XX
6-7	Minute	I2	XX
8-9	Seconds	I2	XX
10-14	Geoc. Lat.	F5.1	+XX.X
15-19	West Long.	F5.1	XXX.X
20-26	Alt. at Perigee (km)	F7.2	XXXX.XX
27-35	Density at Perigee	E9.3	X.XXXE-XX
36-44	Density at Std. Height	E9.3	X.XXXE-XX
45-51	Alt. at 1/2 Scale Ht. (km)	F7.2	XXXX.XX
52-60	Density at 1/2 Scale Ht.	E9.3	X.XXXE-XX
61-66	Model Factor	F6.3	XX.XXX
67-70	Time Span Used - Hours	F4.1	XX.X
71-72	Atmospheric Model Used	I2	XX
73-76	Standard Error of Differential Correction	F4.2	X.XX

1.2.4.8 BADMEP Input

The run control parameters are read through the NAMELIST group NEWINX if columns 61-64 of the device control card contains a one, or the NAMELIST group NEWIN if it contains any other value. The two NAMELIST groups contain the same variables except that NEWIN contains the elements ELM(1) - ELM(6) and NEWINX contains the position and velocity PVOZ(1) - PVOZ(6). The other parameters are as described for NEWIN in Reference 2, except for the expansion of the gravity model arrays C and S, as in CADNIP, and an additional parameter IDC, a numerical code required by the current AFGL system to indicate the plotting device to be used. For definition of this code the user should consult the latest AFGL User's Guide and systems bulletins. The gravity coefficients C_{nm} and S_{nm} are to be read into the arrays C and S as follows:

$$C_{nm}: \quad C \left[n(n + 1)/2 + m - 2 \right]$$

$$S_{nm}: \quad S \left[n(n - 1)/2 + m - 1 \right]$$

The density models available, and their identifying codes, to be input to MODTYP, are the same as just described for CADNIP.

1.3 Neglect of Minor Constituents

The Jacchia-Bass³, Jacchia 1977²⁶, and MSIS^{8,9,31} density models are detailed composition models requiring the computation of the densities of 6 or 7 constituents. If only the total mass density is desired, a significant savings may be made by omitting computation of minor constituents. A study was made of the relative importance of the various constituents in the Jacchia-Bass model for height range 120 km - 1000 km and the temperature range 1500 K - 1900 K in increments of 10 km and 100 K. An algorithm was set up to indicate, at each height and temperature, which constituents could be neglected leaving a total mass density error of 1%. Based on these results the various constituents may be neglected over the following height and temperature ranges:

$$O_2: h \geq 250 + 0.3 (T-500)$$

$$O : h \geq 630 + 1.2 (T-500)$$

$$N_2: h \geq 360 + 0.6 (T-500)$$

N : all heights

$$He: h \leq 240 + 0.2 (T-500)$$

Ar: all heights

$$H: h \leq 330 + 0.6 (T-500)$$

where h is the height in km and T is the exospheric temperature in K, These modifications lead to a 30% reduction in CP time.

A further 13% reduction was gained by substituting in-line code for one-dimensional interpolation in place of calls to a general purpose one-and two-dimensional interpolation routine. Two-dimensional interpolation is not used as often as in the original Jacchia 1977 model because tables are replaced by their analytic representation over most of the height range.

1.4 Satellite Accelerometer Data Studies

Satellite-borne accelerometers designed by AFGL scientists have been the source of plentiful in-situ neutral density measurements in the lower thermosphere. In addition to recent new triaxial accelerometers, flown during periods of moderate and high solar activity⁵, an extensive data base has been compiled³³ from four earlier designed single axis systems flown on satellites S3-1, AE-C, AE-D, and AE-E during the preceding solar cycle. This data base has been used for evaluation of recent density models and development of an empirical global density model³⁴. The more recent triaxial accelerometers provide the opportunity to extend the earlier studies to the higher solar activity peak of the current cycle. In contrast to the earlier instruments, they provide data continuously for extended periods of time. Consequently more detailed studies can be made of thermospheric response to geomagnetic activity.

In addition, 5 months of continuous data from a rotating single axis accelerometer⁶ has become available which, when supplemented by the triaxial accelerometer data, makes possible detailed studies of the latitudinal behavior of the semiannual variation below 220 km.

The difficulty in precisely representing thermospheric dynamics stems from a lack of sufficiently available and representative solar and geomagnetic indices as well as a need for understanding the physics of this region. Studies emphasizing the global specification of densities to meet specific accuracy requirements and provide inputs for specific missions are being made. This entails statistical evaluation of the accuracy of existing models, using available data; incorporation of simple mathematical fixes, when appropriate and feasible, to the model(s) chosen for the density specification; and assessment of the accuracy of the densities so specified.

Section 1.4.1 will discuss software developed to construct data bases for use in evaluation of existing density models. These include data, the corresponding density model values, and data-to-model ratios. Section 1.4.2 discusses software which uses these data bases to perform comparative statistical evaluations of models. Lastly Section 1.4.3 discusses construction of normalized data bases for study of the semiannual variation.

1.4.1 Data Bases for Density Model Evaluation

AFGL scientists, with analytic support from RMY, reduce the raw accelerometer data to densities and construct a data base (Table 4) which includes, for each sample, the Greenwich and local times, geographic and geomagnetic coordinates, solar and geomagnetic activity indices, and Jacchia 1971 model evaluative information (model density and ratio of measured density to model density).

Program FOURMOD has been written to provide evaluative information for up to four CADNIP models selected from Table 5. Program DENDB, discussed later, performs a similar function for the MSIS 77, MSIS 78 and Jacchia 1977 models. The density model package of CADNIP has been modified to compute up to 4 of these models in parallel in a single run. Due to memory requirements, a single run can accommodate no more than two models which require storage of the density tables referred to in Section 1.2.4.5 of this report and Section A.3 of Reference 2. The only exception to this is when models 1 and 2 are selected; since they use the same table, a third model using a table may then be selected. The density tables are assumed to be stored on a master BCD file, TAPE5, similar to that used as a "system file" by program CADNIP (Reference 2, Section A.8). The user controls the copying of selected segments of this file onto TAPES 1-4 with a device control card similar to that described in Reference 2, Section A.8.

Table 4 Accelerometer Density Data Base

Header Record (1 per file)		
Word	Description	Format
0.1	Word Count (40)	I
0.2	Group Count (1)	I
1	Satellite ID	A
2	Experiment Name	A
3	Altitude (km)* or Blank**	I
4-40	Unused	

Data Records (1 or more per file)

Word	Description	Format
0.1	Word Count (40)	I
0.2	Group Count (12)	I
1	Orbit Number	I
2	Date - YYDDD	I
3	GMT - Total Seconds	I or F
4	GMT - Hours	I or F
5	GMT - Minutes	I or F
6	GMT - Seconds	I or F
7	Local Time - Hours	I or F
8	Local Time - Minutes	I or F
9	Local Time - Seconds	I or F
10	Leg (U=up, D=down)	A
11	Day/Night (D or N)	A
12	Spun/Dspun (S or D)	A
13	Geographic Latitude (Deg)	F
14	Geographic East Longitude (Deg)	I or F
15	Geomagnetic Latitude (Deg)	F
16	Geomagnetic East Longitude (Deg)	I or F
17	Invariant Latitude (Deg) or Blank	F
18	Measured Density (gm/cm ³)	F
19	Jacchia 1971 Model Density (gm/cm ³)	F
20, 21	Unused	

Table 4 (Cont'd.)

Word	Description	Format
22	Ratio (Meas/Jacchia 1971)	F
23, 24	Unused	
25	Daily Average Ap or Blank ***	F
26	Unused	
27	Kp (6.7 hour lag)	F
28	F _{10.7} (1 day lag)	F
29	F _{10.7} (3-solar-rotation average)	F
30	Altitude (Km)** or Blank*	F
31-40	Unused	

Words 1-40 repeat for remaining 11 groups. End-of-file separates files; double end-of-file follows last file.

* Altitude Data Base; **Time Data Base; ***Daily Average Ap required for computation of MSIS models by program FOURMOD

Table 5 Density Models Computed by Program FOURMOD

Indicator	Model
1	Jacchia 1964
2	1966 Supplements
3	Jacchia 1971
4	USSR - Cosmos
5	Jacchia-Walker-Bruce
7	Lockheed/NASA
8	MSIS 77 *
9	1962 U.S. Standard
10	MSIS 78 *
11	DENSEL
12	Jacchia 1970
13	Jacchia 1973

* Word 25 of the input database (Table 4) must contain the daily average Ap.

This card consists of 8 fields, read in 8I4 format, specifying the following:

Field	Description
1	Number of BCD card images to skip on TAPE5 prior to copying to TAPE1
2	Number of BCD card images to copy subsequently from TAPE5 to TAPE1
3	Number of BCD card images to skip subsequently on TAPE5, prior to copying to TAPE2
4	Number of BCD card images to copy subsequently to TAPE2
5,6	Similar to fields 3 and 4, but for creating TAPE3
7,8	Similar to fields 3 and 4, but for creating TAPE4

Although, as previously noted, under current limitations at most 2 of the 4 files so created may subsequently be read by the density model package, FOURMOD has provided 4 files to permit later expansion if memory restrictions become less severe. Following the device control card, two other cards are required as described in Table 6.

The solar and geomagnetic activity file normally used by CADNIP is not required, since most of the information is already on the input data base (Table 4). However the six-solar-rotation average of the daily solar flux F10.7, rather than the three-solar-rotation average, is the preferred estimate of the smoothed solar flux for all Jacchia models³⁵, in spite of the reference to the three-solar-rotation average in early Jacchia model reports (References 21 and 24). Therefore a separate file, TAPE6, is required containing one binary data record consisting of the following:

Table 6 Program FOURMOD Punched Card Input

Card #	Column	Format	Variable	Description
1	Device Control Card (See text)			
2	1-5	I5	NMOD	Number of models to be computed (1,2,3,or 4)
2	6-10	I5	IMOD(1)	Indicator of first model (see text)
2	11-15	I5	NDENTP(1)	Number of file containing tables for first model (0,1,2,3,or 4)
2	16-20	I5	IMOD(2)	
2	21-25	I5	NDENTP(2)	
2	26-30	I5	IMOD(3)	
2	31-35	I5	NDENTP(3)	
2	36-40	I5	IMOD(4)	
2	41-45	I5	NDENTP(4)	
3	1-5	I5	IREPT	Repeat factor for printout of data
3	6-10	I5	IALTDB	Zero indicates time data base; non-zero indicates altitude data base
3	11-15	I5	IORMAG	Zero indicates data words 3-9, 14, 16 are integers; non-zero indicates they are floating point (real)

Word	Variable	Description
1	TSTART	Modified Julian Day of the first day for which smoothed solar flux is provided
2	N	Length of the period, in days, for which smoothed solar flux is provided
3 thru N + 2	FBAR6	Smoothed solar flux (6-solar-rotation averages of daily solar flux) for each day of this period

The data provided on TAPE6 must of course cover at least all times for which density data are given on the input data base.

The input and output data bases are identified as TAPE9 and TAPE10, respectively. Table 7 describes the output data base.

The following differences between the Jacchia 1971 model version provided by FOURMOD (from the CADNIP package) and the original model (Reference 24) provided in the input data base should be noted.

- 1) In the original model there is a break at 200km in the computation of the geomagnetic activity correction: below 200km a hybrid correction is made to the exospheric temperature and to the density (Reference 24), while above 200km only an exospheric temperature correction is computed. The CADNIP (FOURMOD) version uses the hybrid correction at all heights.
- 2) Seasonal-latitudinal corrections for helium are neglected in the CADNIP (FOURMOD) version.

Table 7 Program FOURMOD Output Data Base

Header Record (1 per file)

Copy of input header record

Data Records (1 or more per file)

Copy of input data records with following exceptions:

Words	Description	Format
3-9, 14, 16	Same as Input	F
19	Density for first model (gm/cm ³)	F
20	Density for second model (gm/cm ³)	F
21	Density for third model (gm/cm ³)	F
22	Ratio (Meas/first model)	F
23	Ratio (Meas/second model)	F
24	Ratio (Meas/third model)	F
26	Ap (6.7 hr time lag)	F
37	Density (fourth model, gm/cm ³)	F
38	Ratio (Meas/fourth model)	F

- 3) The original J71 on the input data base is computed with the three solar-rotation average of solar flux, while, as mentioned previously, FOURMOD employs the six-solar-rotation average.

Of these the first difference is probably the most significant, since the models will differ above 200km for moderate and high geomagnetic activity. The helium correction is not expected to be important in the altitude range of interest. The use of different solar flux averaging periods could affect results for moderate to high solar activity.

Table 8 DENDB Output Data Base

Header Record (1 per file)
Copy of input header record

Data Records (1 or more per file)
Copy of input data records, with the following exceptions:

Words	Description	Format
3-9,14,16	Same as input	F
20	Jacchia 1977 model density (gm/cm ³)	F
21	MSIS 77 model density (gm/cm ³)	F
23	Ratio (meas/Jacchia 1977)	F
24	Ratio (meas/MSIS 77)	F
25	MSIS 78 model density (gm/cm ³)	F
26	Ratio (meas/MSIS 78)	F

Program DENDB constructs similar model evaluation data bases for the Jacchia 1977, MSIS 77 and MSIS 78 density models. It makes use of the density model computation package of program DENMOD³⁶. The input data base (Table 4) must be on TAPE1, while the output data base, summarized in Table 8, is written on TAPE2. The solar and geomagnetic activity tables required by CADNIP are also required by DENDB and must be input through TAPE3. A mass storage file JSDB, required for the Jacchia 1977 model, is described in Table 1, Section 1, of Reference 36.

Density model evaluation data bases have been constructed for the models listed in Table 5 and the Jacchia 1977 model, using data from the AE/S3-1 data base, the rotatable calibration accelerometer (ROCA) and two recently-flown triaxial accelerometers (SETA-1 and SETA-2).

DENSITY MODEL RATIO STATISTICAL SUMMARIES

BIN NO.	KP		LOCAL TIME		GEOGR LAT	
	MIN	MAX	MIN	MAX	MIN	MAX
1	0.0000	3.1000	8.0000	24.0000	-90.0000	-80.0000
2	0.0000	3.1000	8.0000	24.0000	-80.0000	-70.0000
3	0.0000	3.1000	8.0000	24.0000	-70.0000	-60.0000
4	0.0000	3.1000	8.0000	24.0000	-60.0000	-50.0000
5	0.0000	3.1000	8.0000	24.0000	-50.0000	-40.0000
6	0.0000	3.1000	8.0000	24.0000	-40.0000	-30.0000
7	0.0000	3.1000	8.0000	24.0000	-30.0000	-20.0000
8	0.0000	3.1000	8.0000	24.0000	-20.0000	-10.0000
9	0.0000	3.1000	8.0000	24.0000	-10.0000	0.0000
10	0.0000	3.1000	8.0000	24.0000	0.0000	10.0000
11	0.0000	3.1000	8.0000	24.0000	10.0000	20.0000
12	0.0000	3.1000	8.0000	24.0000	20.0000	30.0000
13	0.0000	3.1000	8.0000	24.0000	30.0000	40.0000
14	0.0000	3.1000	8.0000	24.0000	40.0000	50.0000
15	0.0000	3.1000	8.0000	24.0000	50.0000	60.0000
16	0.0000	3.1000	8.0000	24.0000	60.0000	70.0000
17	0.0000	3.1000	8.0000	24.0000	70.0000	80.0000
18	0.0000	3.1000	8.0000	24.0000	80.0000	90.0000
19	3.1000	4.4000	8.0000	24.0000	-90.0000	-80.0000
20	3.1000	4.4000	8.0000	24.0000	-80.0000	-70.0000
21	3.1000	4.4000	8.0000	24.0000	-70.0000	-60.0000
22	3.1000	4.4000	8.0000	24.0000	-60.0000	-50.0000
23	3.1000	4.4000	8.0000	24.0000	-50.0000	-40.0000
24	3.1000	4.4000	8.0000	24.0000	-40.0000	-30.0000
25	3.1000	4.4000	8.0000	24.0000	-30.0000	-20.0000
26	3.1000	4.4000	8.0000	24.0000	-20.0000	-10.0000
27	3.1000	4.4000	8.0000	24.0000	-10.0000	0.0000
28	3.1000	4.4000	8.0000	24.0000	0.0000	10.0000
29	3.1000	4.4000	8.0000	24.0000	10.0000	20.0000
30	3.1000	4.4000	8.0000	24.0000	20.0000	30.0000
31	3.1000	4.4000	8.0000	24.0000	30.0000	40.0000
32	3.1000	4.4000	8.0000	24.0000	40.0000	50.0000
33	3.1000	4.4000	8.0000	24.0000	50.0000	60.0000
34	3.1000	4.4000	8.0000	24.0000	60.0000	70.0000
35	3.1000	4.4000	8.0000	24.0000	70.0000	80.0000
36	3.1000	4.4000	8.0000	24.0000	80.0000	90.0000
37	4.4000	9.1000	8.0000	24.0000	-90.0000	-80.0000
38	4.4000	9.1000	8.0000	24.0000	-80.0000	-70.0000
39	4.4000	9.1000	8.0000	24.0000	-70.0000	-60.0000
40	4.4000	9.1000	8.0000	24.0000	-60.0000	-50.0000
41	4.4000	9.1000	8.0000	24.0000	-50.0000	-40.0000
42	4.4000	9.1000	8.0000	24.0000	-40.0000	-30.0000
43	4.4000	9.1000	8.0000	24.0000	-30.0000	-20.0000
44	4.4000	9.1000	8.0000	24.0000	-20.0000	-10.0000
45	4.4000	9.1000	8.0000	24.0000	-10.0000	0.0000
46	4.4000	9.1000	8.0000	24.0000	0.0000	10.0000
47	4.4000	9.1000	8.0000	24.0000	10.0000	20.0000
48	4.4000	9.1000	8.0000	24.0000	20.0000	30.0000
49	4.4000	9.1000	8.0000	24.0000	30.0000	40.0000
50	4.4000	9.1000	8.0000	24.0000	40.0000	50.0000
51	4.4000	9.1000	8.0000	24.0000	50.0000	60.0000
52	4.4000	9.1000	8.0000	24.0000	60.0000	70.0000
53	4.4000	9.1000	8.0000	24.0000	70.0000	80.0000
54	4.4000	9.1000	8.0000	24.0000	80.0000	90.0000

Figure 2. Program STAT Sample: Three Dimensional Bins

Table 9 Punch Card Input for Program STAT

Card #	Column	Format	Variable(s)	Description
1	1	I1	IALTOB	0 for time data base 1 for altitude data base
1	6-10	I5	ALTMN	Minimum altitude to process
1	11-15	I5	ALTMX	Maximum altitude to process
2	1-30	3A10	Var (1), Var (2), Var (3)	BCD (10 character) names of up to 3 variables to be used to define bins. If a blank name is given, only the non- blank names preceding it will be considered.
3	1-40	4A10	DENHED (1), DENHED (2), DENHED (3), DENHED (4)	BCD names of the density models (up to 4) to be processed. A blank name has the same effect as for VAR in card 2.
3	41-60	4I5	IWD(1), IWD(2), IWD(3), IWD(4)	Word numbers, on data base (Tables 6,8), where the corresponding model ratios are stored.
4+: 1 set of cards per variable named in card 2				
4A	1-5	I5	IVARN (I)	Word number on data base where the value of the Ith variable is stored
4A	6-10	I5	NBIN (I)	Number of bins for this variable (24 maximum)
4B	1-80	8F10.3	((AMINMX(J,K,I) J=1,2) K=1, NBIN), DEFMNMX(1,I), DEFMNMX(2,I)	AMINMX: Minimum and maximum values of Ith variable per bin. DEFMNMX: Default minimum and maximum values for Ith variable
5	1-3	3I1	IBNFLG (1), IBNFLG (2), IBNFLG (3)	Bin flags for the variables named in card 2 (see text). Several cards may be input, terminated by a card of all zeroes.

Card 4B may be continued as necessary.

Table 10. Sample Bin Specification for Program STAT

Variable	No. of Bins	Minima	Maxima	Default Minimum	Default Maxima
KP	3	0.0	3.1	0.0	9.1
		3.1	4.4		
		4.4	9.1		
Local Time (Hrs.)	1	8	24	8	24
Geographic Latitude (Deg.)	18	-90.0	-80.0	-90.0	90.0
		-80.0	-70.0		
		-70.0	-60.0		
		-60.0	-50.0		
		-50.0	-40.0		
		-40.0	-30.0		
		-30.0	-20.0		
		-20.0	-10.0		
		-10.0	0.0		
		0.0	10.0		
		10.0	20.0		
		20.0	30.0		
		30.0	40.0		
		40.0	50.0		
		50.0	60.0		
		60.0	70.0		
		70.0	80.0		
		80.0	90.0		

1.4.2 Statistical Evaluation of Density Models

Statistical evaluation of density models has been performed by computation of the mean M and percent standard deviation S from the mean, of the data-to-model ratio:

$$M = \frac{\sum_{i=1}^N R_i}{N}$$

$$S = \frac{100}{M} \sqrt{\frac{\sum_{i=1}^N (R_i - M)^2}{N-1}}$$

where

R_i = data to model ratio for the i th sample

N = number of samples

The data are typically sorted into bins defined by 1-3 variables in the data base.

In some instances, particularly when a large set of models is under examination, only a single overall evaluation is desired.

The division of data into bins permits one to compare the effectiveness of various models as certain conditions such as latitude, height, local time or geomagnetic activity are varied. A significant variation of a model's mean ratio over the range of some parameter, such as latitude, would indicate a deficiency of the model in its dependence on that

variable. Large standard deviations often are caused by failure to include some variable in the model. A typical example is the high standard deviations often encountered at high latitudes. This is presumably caused by poor modeling of heating at these latitudes, or what is more often said, the lack of a simple index, or indices, which adequately represent(s) the dynamics of such high latitude effects as particle precipitation and joule heating. Unmodelled density waves are also sources of high standard deviations.

Program STAT has been developed to provide these statistical evaluation capabilities. Table 9 summarizes the punched card input required to operate this program. As indicated in the card 2 input, up to three variables (such as geocentric latitude, or local time) may be used to define bins. STAT will count only those variables named before the first blank 10 column field on card 2. If the first field is blank then all the data within the altitude limits defined on card 1 is handled as one group. In this special case there is no binning, and cards 4 and 5 are not required. A similar technique is used by STAT in reading card 3 to determine the number of models to be processed. However in this case a blank field in columns 1-10 triggers an error termination (there must be at least one model).

A detailed explanation of input cards 4 and 5 is given here. The user may submit as many bin flag cards as desired, terminating with all zeroes. Each card will generate all possible bins with minimum and maximum pairs specified by the array AMINMX for each variable whose flag is odd, and specified by the array DEFMINMX for each variable whose flag is even. Suppose, for example, we are binning with respect to KP, local time and latitude and have specified the bin minima and maxima for each variable as in Table 10. Then the bin structure defined by flags 1, 0, 1 would be as shown in Figure 2. If the total number of bins constructed by all bin flag cards exceeds 300, an error message is written and the program terminates.

The specification of altitude minimum and maximum on card 1 appears unnecessary at this point. However due to increasing uncertainty in the data at high altitudes it is often desired to limit the altitude range of the data to be considered, even when the altitude is not being used as a bin variable. In such cases the input on card 1 avoids the necessity of superficially using the altitude as one of the variables defining bins.

Figure 3 shows a sample printout of the results for the sample case described in Table 10. Some bins have no samples and thus the results are zeroed. The characteristic trend toward high standard deviations (high density variability) at high latitudes is evident for all levels of geomagnetic activity. Variations of the model ratios with latitude and geomagnetic activity are also present. The Jacchia 1977 model exhibits the most pronounced deviations in ratio from unity, indicating that its response to increase in geomagnetic activity is higher than the measured response in both equatorial and polar regions.

1.4.3 Studies of the Semiannual Variation

The accelerometer measurements present an opportunity for detailed study of the semiannual variation at low altitudes. The Jacchia 1971 model, based mainly on analysis of satellite drag above 200 km, predicts an altitude dependence but no latitudinal dependence. It would therefore be of interest to determine if the lack of latitudinal dependence holds also for the accelerometer data, and if the magnitude of the semiannual variation agrees with that extrapolated downward from the higher altitude results via the Jacchia 1971 model.

DENSITY MODEL RATIO STATISTICAL SUMMARIES

NO. OF POINTS	KP	SATELLITE LOCAL TIME		GEOGR LAT		JACCHIA 71		JACCHIA 77		MSIS 77		MSIS 78	
		MIN	MAX	MIN	MAX	MIN	MAX	AVE	PCT STD	AVE	PCT STD	AVE	PCT STD
0	0.0000	3.1000	8.0000	24.0000	-90.0000	-90.0000	0.0000	0.0000	0.0000	0.0000	0.0000	0.0000	0.0000
0	0.0000	3.1000	8.0000	24.0000	-80.0000	-70.0000	0.0000	0.0000	0.0000	0.0000	0.0000	0.0000	0.0000
0	0.0000	3.1000	8.0000	24.0000	-70.0000	-60.0000	0.0000	0.0000	0.0000	0.0000	0.0000	0.0000	0.0000
0	0.0000	3.1000	8.0000	24.0000	-60.0000	-50.0000	0.0000	0.0000	0.0000	0.0000	0.0000	0.0000	0.0000
151	0.0000	3.1000	8.0000	24.0000	-50.0000	-40.0000	1.0302	7.0411	.9865	9.1373	.9026	8.7973	.8911
660	0.0000	3.1000	8.0000	24.0000	-40.0000	-30.0000	1.0097	6.7213	.9510	7.5332	.8929	7.0381	.8914
992	0.0000	3.1000	8.0000	24.0000	-30.0000	-20.0000	.9867	6.0674	.9194	7.5194	.9127	7.0216	.9099
1003	0.0000	3.1000	8.0000	24.0000	-20.0000	-10.0000	.9461	7.1337	.8771	7.5683	.9368	6.8406	.9341
1037	0.0000	3.1000	8.0000	24.0000	-10.0000	0.0000	.9407	7.0095	.8700	8.0979	.9633	6.0476	.9621
1125	0.0000	3.1000	8.0000	24.0000	0.0000	10.0000	.9674	8.7466	.8988	8.3294	.9837	5.5008	.9857
1207	0.0000	3.1000	8.0000	24.0000	10.0000	20.0000	1.0063	9.9582	.9460	8.8840	.9917	7.3058	.9977
1333	0.0000	3.1000	8.0000	24.0000	20.0000	30.0000	1.0333	10.4981	.9904	8.7136	.9984	8.0001	1.0007
1515	0.0000	3.1000	8.0000	24.0000	30.0000	40.0000	1.0245	10.1935	1.0036	8.6342	.9905	8.0385	.9905
1617	0.0000	3.1000	8.0000	24.0000	40.0000	50.0000	1.0051	8.6781	.9988	7.3638	.9732	7.5611	.9722
1674	0.0000	3.1000	8.0000	24.0000	50.0000	60.0000	.9840	6.7243	.9801	6.1621	.9572	6.3196	.9562
1829	0.0000	3.1000	8.0000	24.0000	60.0000	70.0000	.9814	7.7317	.9622	7.6794	.9597	7.9666	.9594
2136	0.0000	3.1000	8.0000	24.0000	70.0000	80.0000	.9673	8.9211	.9292	9.5833	.9557	8.7001	.9571
1516	0.0000	3.1000	8.0000	24.0000	80.0000	90.0000	.9559	10.3599	.9039	10.5685	.9473	10.2509	.9487
0	3.1000	4.4000	8.0000	24.0000	-90.0000	-80.0000	0.0000	0.0000	0.0000	0.0000	0.0000	0.0000	0.0000
0	3.1000	4.4000	8.0000	24.0000	-80.0000	-70.0000	0.0000	0.0000	0.0000	0.0000	0.0000	0.0000	0.0000
0	3.1000	4.4000	8.0000	24.0000	-70.0000	-60.0000	0.0000	0.0000	0.0000	0.0000	0.0000	0.0000	0.0000
0	3.1000	4.4000	8.0000	24.0000	-60.0000	-50.0000	0.0000	0.0000	0.0000	0.0000	0.0000	0.0000	0.0000
64	3.1000	4.4000	8.0000	24.0000	-50.0000	-40.0000	1.0208	5.9349	.9969	8.8725	.9305	9.1074	.9169
196	3.1000	4.4000	8.0000	24.0000	-40.0000	-30.0000	1.0072	6.0206	.9381	8.1846	.9244	8.0000	.9177
313	3.1000	4.4000	8.0000	24.0000	-30.0000	-20.0000	.9695	6.5116	.8881	9.8867	.9367	7.2199	.9298
323	3.1000	4.4000	8.0000	24.0000	-20.0000	-10.0000	.9288	6.0713	.8289	9.2818	.9662	6.3015	.9601
339	3.1000	4.4000	8.0000	24.0000	-10.0000	0.0000	.9051	6.0464	.8065	8.7470	.9852	6.4031	.9824
363	3.1000	4.4000	8.0000	24.0000	0.0000	10.0000	.9388	11.0458	.8418	10.1524	1.0103	7.2812	1.0125
375	3.1000	4.4000	8.0000	24.0000	10.0000	20.0000	.9813	11.2856	.9087	9.3638	1.0257	8.5508	1.0328
448	3.1000	4.4000	8.0000	24.0000	20.0000	30.0000	1.0002	12.1468	.9574	10.0327	1.0307	9.0138	1.0373
460	3.1000	4.4000	8.0000	24.0000	30.0000	40.0000	1.0041	11.1248	.9999	8.7933	1.0263	9.7718	1.0297
503	3.1000	4.4000	8.0000	24.0000	40.0000	50.0000	.9876	9.5683	1.0101	8.9371	1.0056	8.7471	1.0069
552	3.1000	4.4000	8.0000	24.0000	50.0000	60.0000	.9865	8.4155	1.0056	9.2440	1.0039	8.3005	1.0054
630	3.1000	4.4000	8.0000	24.0000	60.0000	70.0000	.9886	9.7081	.9740	11.3591	1.0063	11.4071	1.0079
696	3.1000	4.4000	8.0000	24.0000	70.0000	80.0000	.9718	11.8757	.9264	14.3950	.9946	13.5157	.9950
490	3.1000	4.4000	8.0000	24.0000	80.0000	90.0000	.9313	14.2865	.8692	16.1738	.9555	14.5902	.9569
0	4.4000	9.1000	8.0000	24.0000	-90.0000	-80.0000	0.0000	0.0000	0.0000	0.0000	0.0000	0.0000	0.0000
0	4.4000	9.1000	8.0000	24.0000	-80.0000	-70.0000	0.0000	0.0000	0.0000	0.0000	0.0000	0.0000	0.0000
0	4.4000	9.1000	8.0000	24.0000	-70.0000	-60.0000	0.0000	0.0000	0.0000	0.0000	0.0000	0.0000	0.0000
0	4.4000	9.1000	8.0000	24.0000	-60.0000	-50.0000	0.0000	0.0000	0.0000	0.0000	0.0000	0.0000	0.0000
59	4.4000	9.1000	8.0000	24.0000	-50.0000	-40.0000	.9689	6.8904	.8977	12.1527	.8647	7.5526	.8664
191	4.4000	9.1000	8.0000	24.0000	-40.0000	-30.0000	.9891	7.3866	.8718	11.9604	.8956	9.8028	.8952
263	4.4000	9.1000	8.0000	24.0000	-30.0000	-20.0000	.9306	7.7078	.7914	13.1799	.9091	8.6253	.9113
262	4.4000	9.1000	8.0000	24.0000	-20.0000	-10.0000	.8796	8.7967	.7195	14.7476	.9485	9.1550	.9520
290	4.4000	9.1000	8.0000	24.0000	-10.0000	0.0000	.8917	13.2248	.7036	14.5667	.9928	8.4785	.9938
290	4.4000	9.1000	8.0000	24.0000	0.0000	10.0000	.9069	14.5875	.7154	15.2590	1.0069	8.5500	1.0042
263	4.4000	9.1000	8.0000	24.0000	10.0000	20.0000	.9242	14.6419	.7691	16.0476	1.0110	8.9674	1.0058
278	4.4000	9.1000	8.0000	24.0000	20.0000	30.0000	.9534	13.6305	.8634	15.0849	1.0262	10.7081	1.0243
374	4.4000	9.1000	8.0000	24.0000	30.0000	40.0000	.9737	13.0364	.9275	13.3576	1.0190	11.3253	1.0189
428	4.4000	9.1000	8.0000	24.0000	40.0000	50.0000	.9597	12.1767	.9309	13.0134	.9791	11.0757	.9781
452	4.4000	9.1000	8.0000	24.0000	50.0000	60.0000	.9628	11.5255	.9001	16.5522	.9593	13.3277	.9571
467	4.4000	9.1000	8.0000	24.0000	60.0000	70.0000	.9435	11.7343	.8349	20.6822	.9327	14.7411	.9279
529	4.4000	9.1000	8.0000	24.0000	70.0000	80.0000	.9305	11.0268	.7805	21.2561	.9259	15.4667	.9148
386	4.4000	9.1000	8.0000	24.0000	80.0000	90.0000	.9158	12.7364	.7538	24.7591	.9228	18.6561	.9068

Figure 3. Sample Program STAT Output

The best data base constructed thus far is the ROCA data base, which includes continuous coverage from day 89 to day 223, in 1978. This therefore includes the April maximum and the July minimum. Data covering later portions of a year may be available shortly.

Figure 4 summarizes the software system that has been developed to support this study. Program BNSORT accepts as input any data base prepared by Program FOURMOD (Table 7) or DENDB (Table 8). Given bin parameter and normalization specifications (Table 11), it constructs a bin-sorted data base of densities (Table 12) normalized to approximately remove all variations except the semiannual. The normalized densities are computed by

$$d_n = R d_{mod}$$

where d_n is the normalized density, R is the measured to model ratio on the input data base, and d_{mod} is the model value for the specified normalization parameters: altitude, latitude, local time, solar activity and geomagnetic activity, and with the solar declination set to zero regardless of the time of year. Program DAILAV constructs, from this, an output data base (Table 13) containing the daily averaged normalized densities. Program SUADB formats these into a file compatible with AFGL's interactive graphics program, SUATEK.

Figure 5 shows some sample results. Despite the scatter in the data, the semiannual variation appears to be nearly the same at all latitudes. There is some indication that it may be smaller than that predicted by the Jacchia 1971 model, as shown in Table 14. It must be emphasized that these are preliminary findings subject to change as more data become available.

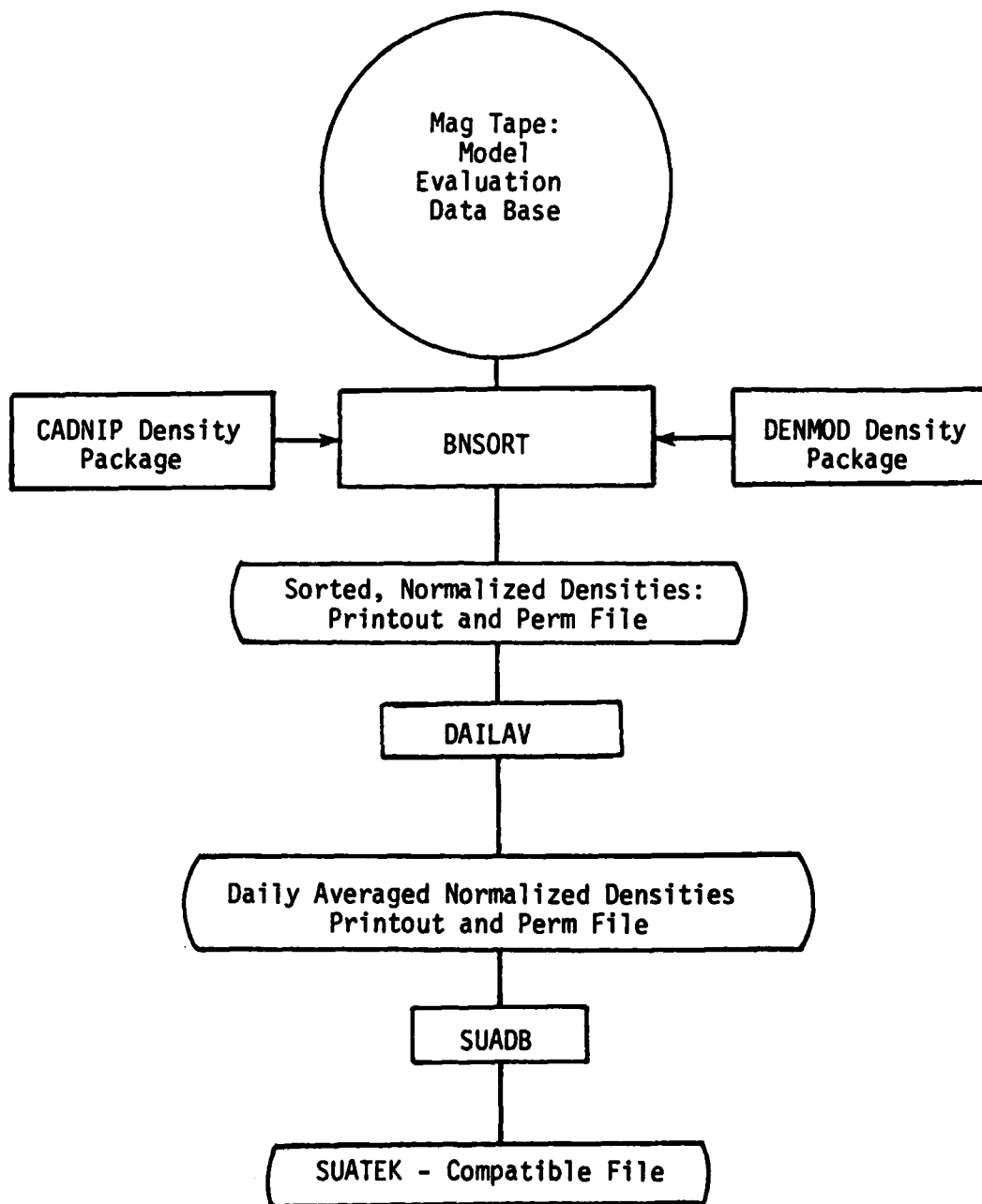


Figure 4. Software for Studying the Semiannual Variation

63-4 NORMALIZED TO JACCHIA 71 F10-160 KP=2.0

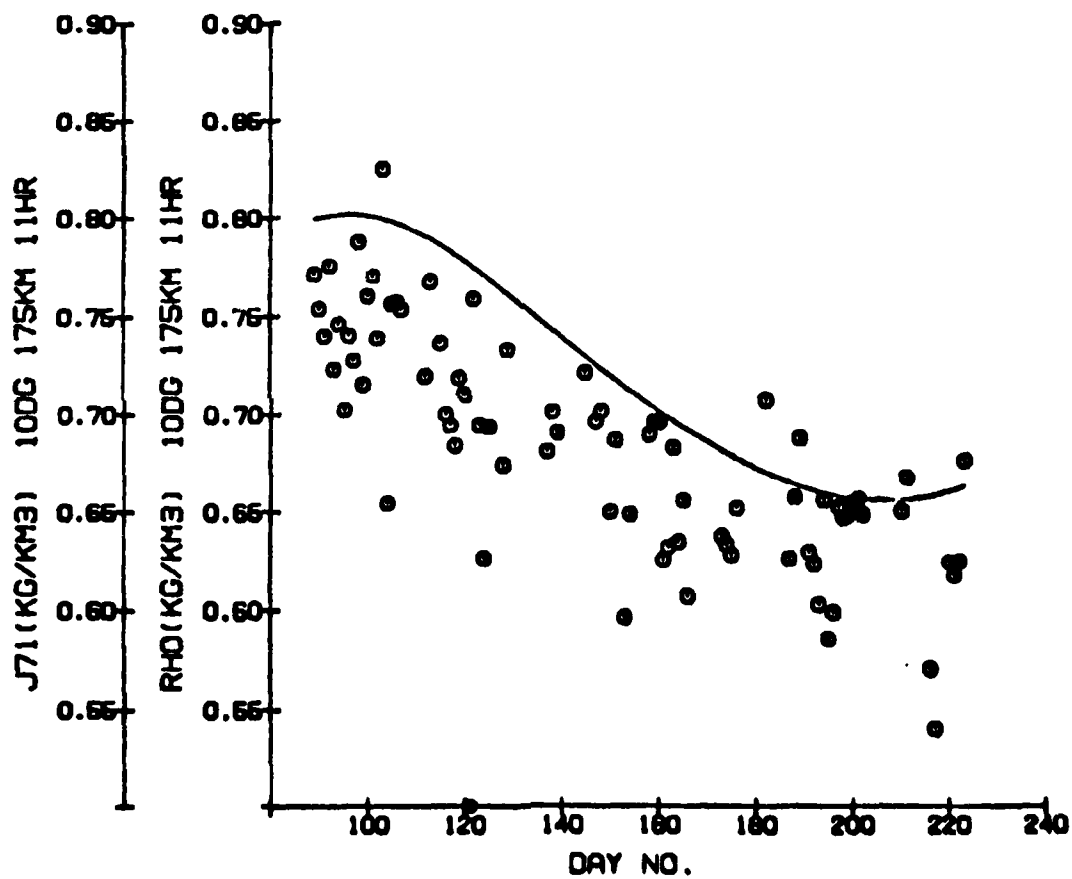


Figure 5. Sample of Normalized Data for the Semiannual Variation. The symbols represent data points while the curve indicates the Jacchia 1971 Model.

Table 11. Program BNSORT Input

```

PROGRAM BNSORT (INPUT=65,CU1PUT=65,TAPE1=520,TAPE2=520,TAPE3=520,
  TAPE4=65)
  SORTS A DENSITY DATA BASE INTO LATITUDE-LOCAL TIME BINS.
  THE DATA IN EACH BIN ARE THEN NORMALIZED TO A SPECIFIC
  LATITUDE, ALTITUDE, AND LOCAL TIME

INPUTS
CARD          VARIABLE          CCL          FORMAT          DESCRIPTION
1             N3INS             1-5           I5              NO. OF BINS
1             OLAT              11-20        F10.3           LATITUDE
                     WIDTH
2 + (ONE CARD PER BIN)
              CLAT              1-10          F10.3           NORMALIZING LAT
              ALOC1             11-20        F10.3           MIN. LOC. TIME
              ALOC2             21-30        F10.3           MAX. LOC. TIME
              CLOC              31-40        F10.3           NORMALIZING L. T.
              CALT              41-50        F10.3           NORMALIZING ALT
3             CF1CP7            1-10          F10.3           NORMALIZING F10.7
3             CKP               11-20        F10.3           NORMALIZING KE
3             IMCC              21-25          I5             NORMALIZING DENSITY
                     MCDL
3             IMOC1             26-30          I5             DENSITY MODEL PACKAGE
                     (SEE BELOW)
IMOC AND IMCC1 DETERMINE THE DENSITY MODEL TO BE USED
AS FOLLOWS
IMOC1 = 0 (DENMCO PACKAGE)
IMCC=1    NOT ALLOWED
IMCC=2    JACCHIA 1977
IMCC=3    MSIS 77
IMCC=4    MSIS 78
IMOC1 = 1 (CAGNIP PACKAGE)
IMOC=1    JACCHIA 1964
IMOC=2    US STAND 1966
IMOC=3    JACCHIA 1971
IMOC=4    USSR-CCSMOS
TAPE1 INPUT DATA BASE
TAPE4 DENSITY TABLES (NEEDED FOR CAGNIP PACKAGE)

```

Table 12. Program BNSORT Output

```

OUTPUTS
TAPE3 BINARY
1 FILE PER BIN
  HEADER
    1. SATELLITE ID (A)
    2. CLAT (F)
    3. OLAT (F)
    4. ALOC1 (F)
    5. ALOC2 (F)
    6. CLOC (F)
    7. CALT (F)
    8. CF1CP7 (F)
    9. CKP (F)
    10. NORMALIZING MCDL (A)
    12. NP (TOTAL NUMBER OF FCINS IN BIN) (I)
DATA RECORDS IW,JG,((DATA(I,J),J=1,IW),J=1,JG)
            IW=5,JG=127
            DATA(1,J) = TIME (YEARS+FRACTION OF DAY)
            DATA(2,J) = ORBIT NUMBER
            DATA(3,J) = MEASURED DENSITY
            DATA(4,J) = NORMALIZED DENSITY
            DATA(5,J) = ALTITUDE

```

Table 13. Program DAILAV Input and Output

```

PROGRAM DAILAV (INPLT=65, OUTPUT=65, TAPE1=52 J, TAPE2=52 J)
CONSTRUCTS DAILY AVERAGE NORMALIZED DENSITY DATA BASE FOR LATITUDE/
LOCAL TIME BINS, FROM SAMPLE DATA BASE CONSTRUCTED BY PROGRAM INSORT.
TAPE1 - INPUT DATA BASE---SEE PROGRAM INSORT
TAPE2 - OUTPUT DATA BASE
      ONE FILE PER BIN
      HEADER RECORD - SAME AS FOR INPLT DATA BASE
      DATA RECORDS
      IN, JG, ((ACAT(I, J), I=1, IW), J=1, JG)
      IW=4, MAXIMUM JG=127
      ACATA(1, J) = IYCCC (YEAR AND DAY NUMBER) (INT)
      ACATA(2, J) = DAILY AVERAGED NORMALIZED DENSITY
                   (REAL)
      ACATA(3, J) = STANDARD DEVIATION (REAL)
      ACATA(4, J) = NUMBER OF SAMPLES (INTEGER)

```

Table 14
 Semiannual Variation
 Local Time: 1100 Hrs.
 Altitude: 175 km.

Geographic Latitude (Deg N)	Ratio, April Max/July Min
0	1.14
10	1.11
20	1.15
30	1.13
40	1.11
50	1.10
60	1.09
70	1.13
80	1.22
J71 (all latitudes)	1.22

1.5 References

1. Forbes, J.M., and Garrett, H.B., Theoretical Studies of Atmospheric Tides, Rev. of Geophys. and Space Res., Volume 17, No. 8., pp. 1951 - 1981, 1979.
2. Bramson, A.S., and Slowey, J.W., Some Recent Innovations in Atmospheric Density Programs, AFCRL-TR-74-0370, 1974, AD786414,
3. Bass, J.N., Analytic Representation of the Jacchia 1977 Model Atmosphere, AFGL-TR-80-0037, 1980, ADA085782 .
4. Champion, K.S.W., and Marcos, F.A., The Triaxial Accelerometer System on Atmosphere Explorer, Radio Sci., Volume 8, No. 4, pp. 297 - 303, 1973.
5. Marcos, F.A., and Swift, E.R., Application of the Satellite Triaxial Accelerometer Experiment to Atmospheric Density and Wind Studies, AFGL-TR-82-0091, 1982, ADA120852 .
6. Marcos, F.A., and Champion, K.S.W., Satellite Density Measurements with a Rotatable Calibration Accelerometer (ROCA), AFGL-TR-79-0005, 1979, ADA069740 .
7. Sharp, L.R., Hickman, D.R., Rice, C.J., and Strauss, J.M., The Altitude Dependence of the Local Time Variation of Thermospheric Density, Geophys. Res. Lett., Volume 5, p. 261, 1978.
8. Hedin, A.E., Salah, J.E., Evans, J.V., Reber, C.A., Newton, G.P., Spencer, N.W., Kayser, D.C., Alcayde, D., Bauer, P., Cogger, L., and McClure, J.P., A Global Thermospheric Model Based on Mass Spectrometer and Incoherent Scatter Data MSIS 1. N₂ Density and Temperature, J. Geophys. Res., Volume 82, No. 16, pp. 2139 - 2147, 1977.

9. Hedin, A.E., Reber, C.A., Newton, G.P., Spencer, N.W., Brinton, H.C., and Mayr, H.G., A Global Thermospheric Model Based on Mass Spectrometer and Incoherent Scatter Data MSIS 2. Composition, J. Geophys. Res., Volume 82, No. 16, pp. 2148 - 2156, 1977.
10. Forbes, J.M., and Marcos, F.A., Tidal Variations in Total Mass Density as Derived from the AE - E Mesa Experiment, J. Geophys. Res., Volume 84, No. 1, pp. 31 - 36, 1979.
11. Garrett, H.B., and Forbes, J.M., Tidal Structure of the Thermosphere at Equinox, J. Atm. Terr. Phys., Volume 40, pp. 657 - 668, 1978.
12. Forbes, J.M., Tidal Variations in Thermospheric O, O₂, N₂, Ar, He, and H, J. Geophys. Res., Volume 83, No. A8, pp. 3961 - 3968, 1978.
13. Forbes, J.M., and Marcos, F.A., Seasonal-Latitudinal Tidal Structures of O, N₂, and Total Mass Density in the Thermosphere, J. Geophys. Res., Volume 85, No. A7, pp. 3489-3493, 1980.
14. U.S. Standard Atmosphere 1976, National Oceanic and Atmospheric Administration, National Aeronautics and Space Administration, and United States Air Force, Washington, D.C., 1976.
15. Hong, S.S., and Lindzen, R.S., Solar Semidiurnal Tide in the Thermosphere, J. Atmos Sci., Volume 33, pp. 135 - 153, 1976.
16. Forbes, J.M., and Garrett, H.B., Solar Diurnal Tide in the Thermosphere, J. Atm. Terr. Phys. Volume 33, pp. 2226 - 2241, 1976.
17. Hedin, A.E., Spencer, N.W., Mayr, H.G., and Harris, I., Direct Evidence of Transport Processes in the Thermospheric Diurnal Tide, J. Geophys. Res. Volume 83, No. A7, pp. 3355 - 3357, 1978.
18. Hedin, A.E., Spencer, N.W., and Mayr, H.G., The Semidiurnal and Terdiurnal Tides in the Equatorial Thermosphere from AE-E Measurements, J. Geophys. Res., Volume 85, No. A4, pp. 1787 - 1791, 1980.

19. Lindzen, R.S., and Kuo, H.L., A Reliable Method for the Numerical Integration of a Large Class of Ordinary and Partial Differential Equations, Mon. Weath. Rev., Volume 97, No. 10, pp. 732 - 734, 1969.
20. Richtmyer, R.D., Difference Methods for Initial-Value Problems, Interscience Press, New York, 1957.
21. Jacchia, L.G., New Static Models of the Thermosphere and Exosphere with Empirical Temperature Profiles, Smithsonian Astrophysical Observatory, Special Report Number 313, 1970.
22. Champion, K.S.W., private communication.
23. Liu, J.J.F., France, R.G., and Wackernagel, H.B., An Analysis of the Use of Empirical Atmospheric Density Models in Orbital Mechanics, in Proceedings of a Workshop on Atmospheric Drag, National Oceanic and Atmospheric Administration, Environmental Research Laboratories, Boulder, CO, pp. 31 - 44, 1982.
24. Jacchia, L.G., Revised Static Models of the Thermosphere and Exosphere with Empirical Temperature Profiles, Smithsonian Astrophysical Observatory, Special Report Number 332, 1971.
25. International Business Machines Corp., System/360 Scientific Subroutine Package, Fifth Edition, 1970.
26. Jacchia, L.G., Thermospheric Temperature, Density and Composition: New Models, Smithsonian Astrophysical Observatory, Special Report Number 375, 1977.
27. Abramowitz, M., and Stegun, I.A., Handbook of Mathematical Functions with Formulas, Graphs, and Mathematical Tables, U.S. National Bureau of Standards, Washington, 1964.
28. Aksnes, K., On the Use of the Hill Variables in Artificial Satellite Theory: Brouwer's Theory, Astron. and Astroph., Volume 17, pp. 70 - 75, 1972.

29. Champion, K.S.W., and Gillette, D.F., under preparation.
30. Elyasberg, P.E., Kugaenko, B.V., Synitsyn, V.M., and Voiskovsky, M.I., Upper Atmospheric Density Determination from the Cosmos Satellite Deceleration Results, Space Research, Vol. XII, pp. 727 - 731, 1972.
31. Hedin, A.E., Reber, C.A., Spencer, N.W., and Brinton, H.C., Global Model of Longitude/UT Variations in Thermospheric Composition and Temperature Based on Mass Spectrometer Data, J. Geophys. Res., Volume 84, No. A1, pp 1 - 9, 1979.
32. Garrett, H.B., An Updated Empirical Density Model for Predicting Low Altitude Satellite Ephemerides, AFCRL-TR-75-0158, 1975, ADA010424.
33. Marcos, F.A., McInerney, R.E., and Fioretti, R.W., Variability of the Lower Thermosphere Determined from Satellite Accelerometer Data, AFGL-TR-78-0134, 1978, ADA058982.
34. Marcos, F.A., Gillette, D.F., and Robinson, E.C., A Global Thermospheric Density Model Based on Satellite Accelerometer Data, AFGL-TR-82-0025, 1982, ADA119861.
35. Slowey, J.W., Private Communication.
36. Logicon, Inc., Analysis and Programming for Research in the Physics of the Upper Atmosphere, AFGL-TR-81-0293, 1982, ADA113932.

2.0 Artifacts in SPA Observations of Radio Wave Scintillations

2.1 Introduction

The purpose of the Scintillation Processor A (SPA) radio receiving system is to investigate irregularities in the ionosphere by examining the properties of transionospheric signals originating from satellites in eccentric orbits¹. To provide a stable phase reference required for extracting valid phase measurements, an ultra-stable local oscillator signal is synthesized. The frequency of this source is shifted from time-to-time to accommodate, within the narrow receiver bandwidth, the time-varying Doppler frequency shift characteristic of the received signals. Continuity of phase is preserved during these frequency shifts. A programmable synthesizer driven by a stable reference oscillator is the hardware configuration used to generate these time-varying local oscillator injection signals. The basic receiver architecture is sketched in Figure 1. The processing of the received signals is performed by a software system described in Reference 1.

2.2 Contamination of SPA Signals

In operation, a problem is encountered with the SPA system. A 'scope display in the field of the intensity of the raw received signal reveals an unwanted sinusoidal component riding atop the received signal. Figure 2 illustrates the time-domain manifestation of the effect. Here the rapidly varying, fine-grain structure of the signal intensity is caused by "beating" between the wanted and the contaminating signals. In terms of the processed data, this effect is most clearly manifested in the signal phase and intensity spectrograms, where it appears as an often prominent ledge-like extension to the roll-off portion of the spectrum. Figure 3 illustrates the effect on phase and intensity spectra. An important analysis objective is to obtain the slope of the roll-off of the spectra. Always a nuisance, the contaminant, when very prominent, can thwart the process of slope evaluation. This unwanted energy, dubbed "coherent leakage", is an artifact which results from the particular architecture employed in the SPA receiver.

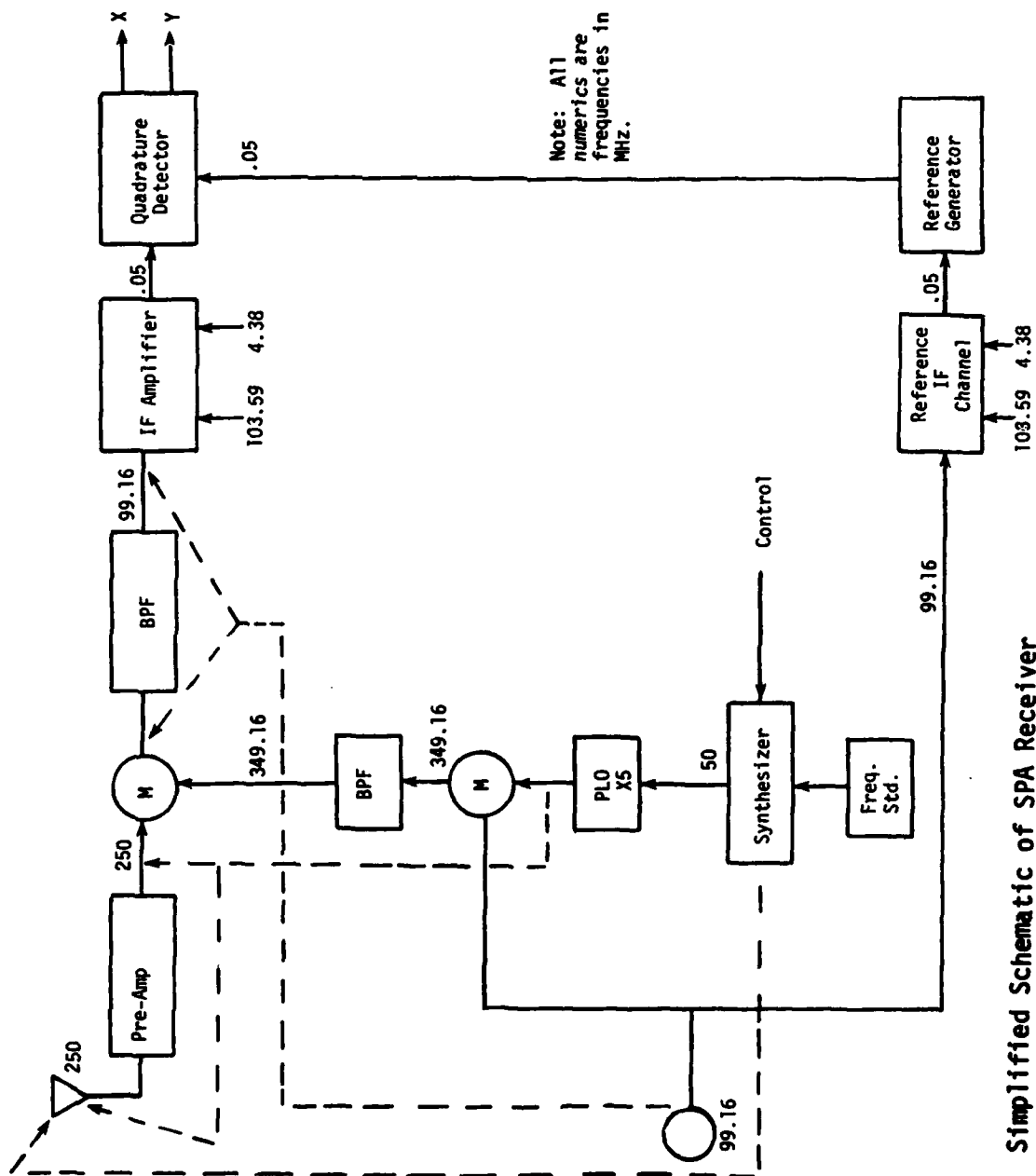


Figure 1. Simplified Schematic of SPA Receiver

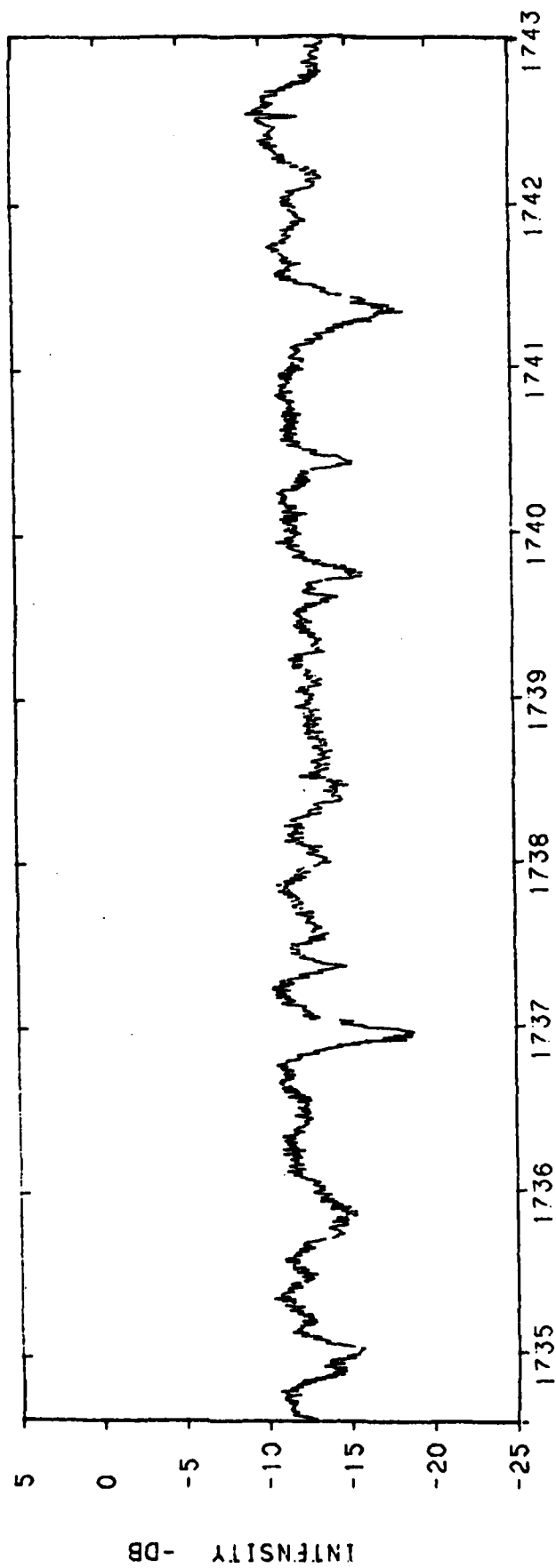
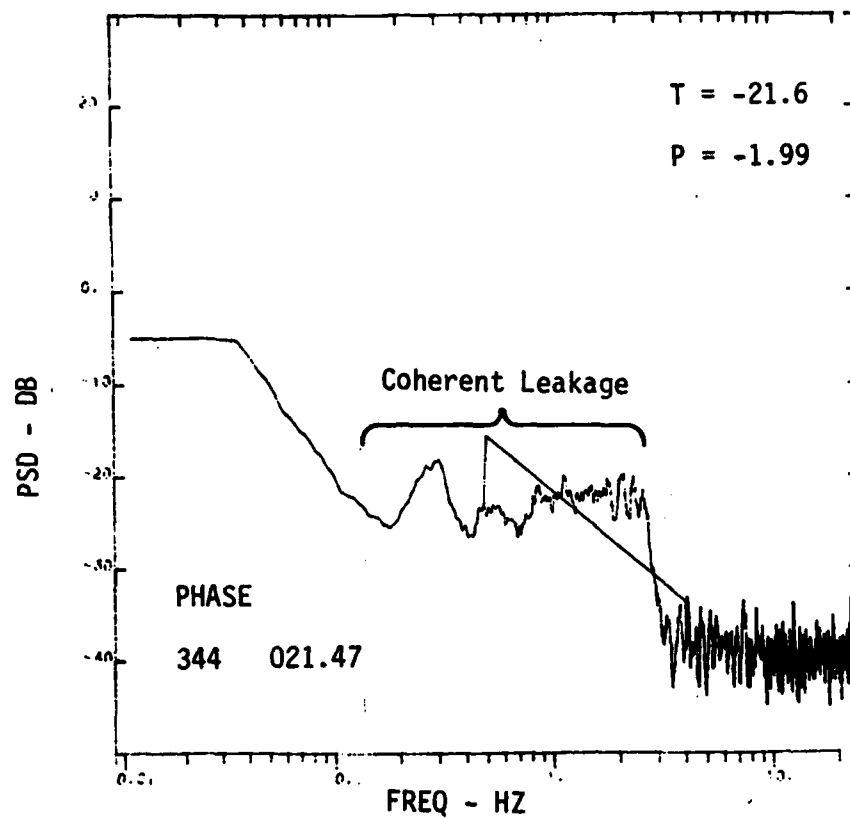
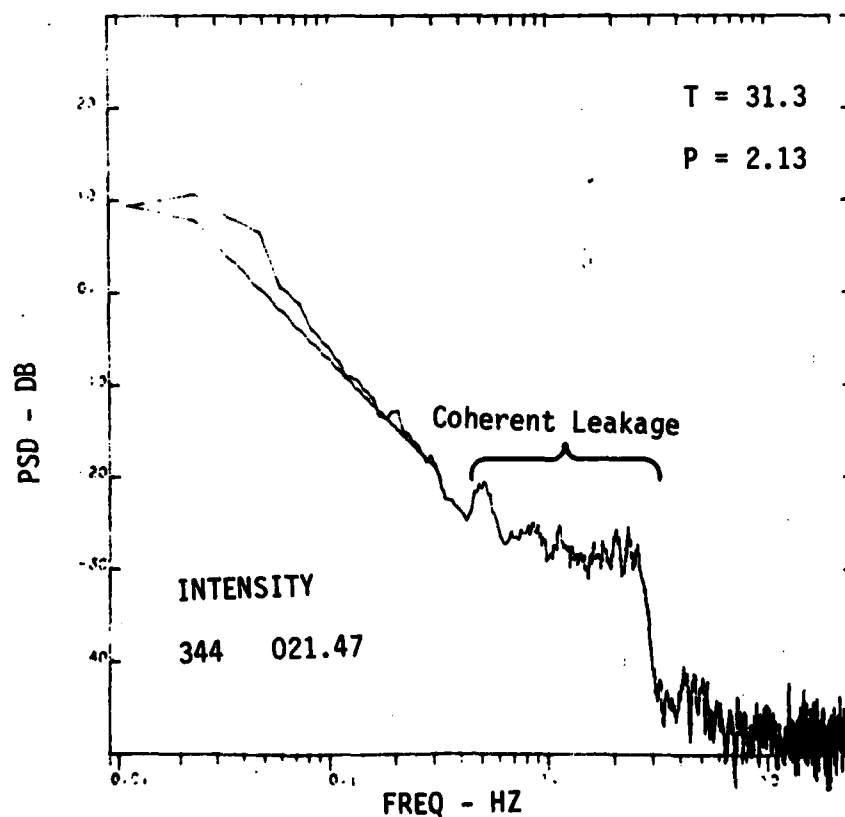


Figure 2. Effect of Coherent Leakage in the Time Domain



a) Intensity Spectrogram



b) Phase Spectrogram

Figure 3. Spectrograms Exhibiting Presence of Coherent Leakage

Examination of the schematic of the SPA receiver (Figure 1) reveals a multiple conversion superheterodyne receiver with a nominal rf input frequency of 250 MHz and a first IF frequency of 99.16 MHz. Notice, particularly, that the frequencies 50, 250, and 99.16 MHz are all generated (at relatively high levels) within the receiving system. Without extreme care with respect to out-of-band rejection for bandpass filters and shielding for both components and interconnecting cables, there is an invitation for these locally-generated frequencies to couple into the signal channel. The dashed lines in Figure 1 are intended to suggest several possible leakage paths. Coherent leakage is the result of some such unwanted coupling. There is some evidence from the field suggesting that the dominant path is one from the synthesizer out to the antenna, coupling 50 MHz energy into the first mixer, where a fifth harmonic is generated. The precise origin, though, is immaterial: with the basic mechanism understood, the task at hand is its elimination, not by hardware modifications, but by special signal processing operations.

At this point the reader may wonder that leakage of an ultra-stable injection frequency at the nominal center frequency (zero Hz reference of the system) should manifest itself as the frequency shifted and spread effect shown in Figure 3. This may be explained as follows:

Assume unit amplitude for the received signal (assumed sinusoidal)

$$s(t) = \sin \omega t$$

Assume an amplitude $a \ll 1$ and frequency $\omega + \delta$ for the leakage

$$l(t) = a \sin \{(\omega + \delta) t + \phi\}$$

The amplitude of the sum of these two can be shown to be approximated by

$$\text{Amplitude} = 1 + a \cos (\delta t + \phi)$$

A spectrogram of the amplitude would show a large d.c. component (the wanted signal) plus a component at the radian "beat" frequency, (the leakage). The dominant component "captures" the zero Hz position, with the lesser component shifted in frequency. A spectrogram of the original raw signal would reverse the situation: independent of relative amplitudes, the coherent leakage component would appear at zero Hz, and the larger wanted signal would show the smearing effect of a changing Doppler frequency shift. It can be understood, now, why the spectrally pure leakage appears spread and frequency shifted: The explanation lies in the phenomenon of capture, coupled with the Doppler drifting and periodic shifting of the signal frequency. That is, the difference frequency between wanted signal and leakage varies with time; and the wanted signal is concentrated near zero Hz. Thus the originally stable leakage has the smeared appearance shown in Figure 3a.

A similar argument could be applied to the case of phase spectra, where again the dominant component captures the zero Hz position.

2.3 Suppression of Leakage

In signal quadrature component space, the leakage represents a transformation of the signal to a new origin. The displacement of the new origin from the old is given by the quadrature components of the leakage. It will be assumed that these components are constant over the signal analysis period ($4096 \text{ samples} \times 1/50 \text{ seconds/sample} = 81.92 \text{ secs}$, see Reference 1). Measurements indicate that the leakage components are, in fact, reasonably constant over such a period. However, there can be appreciable drift from one analysis block to another.

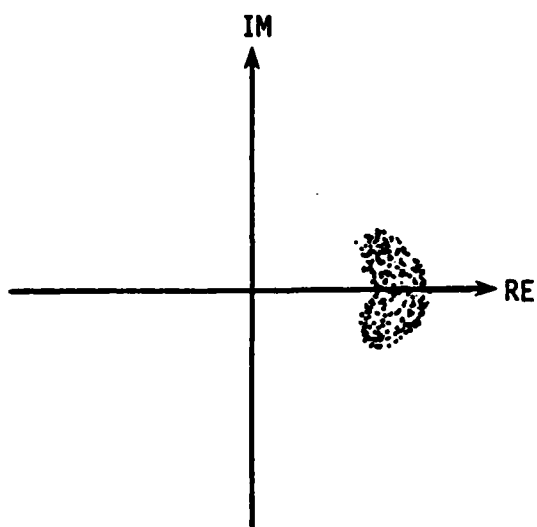
The second assumption to be made is that the received signal has a statistical characterization such that its temporal history, represented in quadrature space, has circular symmetry about the origin. Contributing to the realization of this condition is the fact that the signal is generally offset from the zero-frequency reference by some varying non-zero amount, causing rotation of the signal's phasor representation about the origin.

Now, if the statistics of the signal's phasor representation do not vary with time, it is intuitively obvious that, as this constant pattern undergoes a large number of rotations about the origin, the resultant temporal history of the signal will have circular symmetry. Therefore, we will make the assumption of temporal homogeneity of the statistics of the signal over the 82-second analysis period. This condition appears to be violated only rarely; the usual circumstance is one in which the rate of scintillation is very slow over the analysis period.

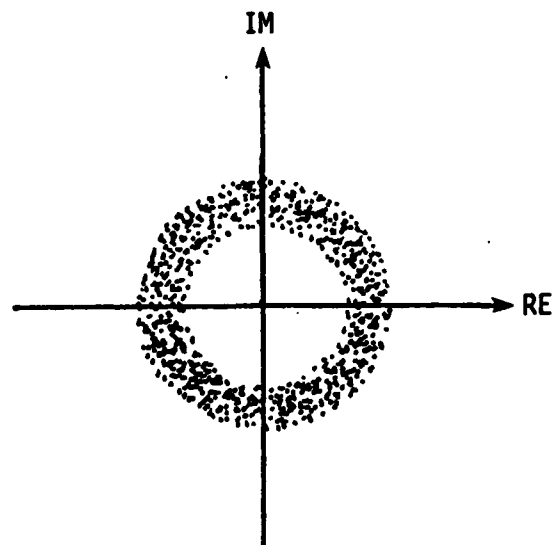
Figure 4a suggests the appearance of the signal scatter plot in quadrature component space under conditions of no coherent leakage and no frequency offset. Temporal homogeneity of the statistics implies that the general pattern of this plot would not change as different time-blocks of data are examined. Figure 4b suggests the effect of having a non-zero frequency offset: the distribution of Figure 4a rotates many times about the origin, yielding a circularly symmetric pattern. Figure 4c illustrates the effect of coherent leakage: the origin (center of symmetry) is shifted. The circular symmetry of the received signal (Figure 4b) implies a zero-mean process. The mean of the process shown in Figure 4c is at the center of symmetry, which is displaced from the origin. The displacement represents the quadrature components of the leakage.

Thus, by forming the mean of the observed signal (Figure 4c) over the 82-second data collections period, we can form a statistical estimate of the coherent leakage signal. The quadrature components of this estimate can then be subtracted from the raw signal to suppress the unwanted leakage and restore the received signal to its natural zero-mean condition.

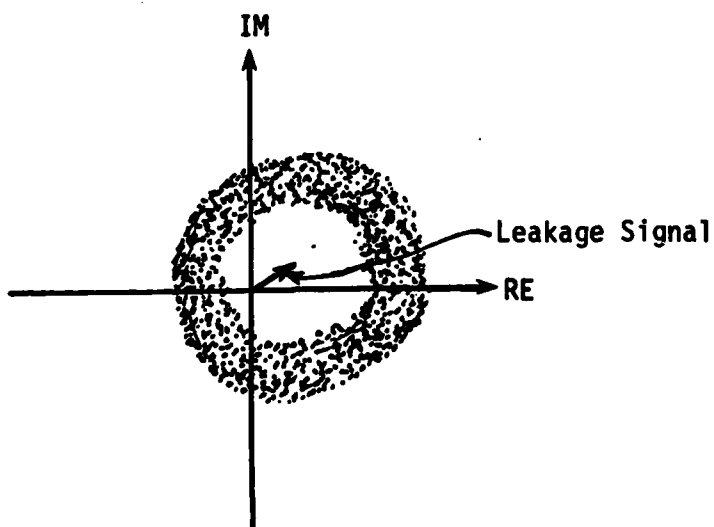
This technique has been implemented in the operational version of the APA processing software. Program TPSCAN unpacks all the data, checks the quality of data, and identifies blocks of data to be processed. For each such block, it forms an estimate of the leakage component, which is stored for use in subsequent processing to suppress the leakage. Figure 5 compares spectra before and after suppression of leakage.



a) Pattern with Zero Offset Frequency

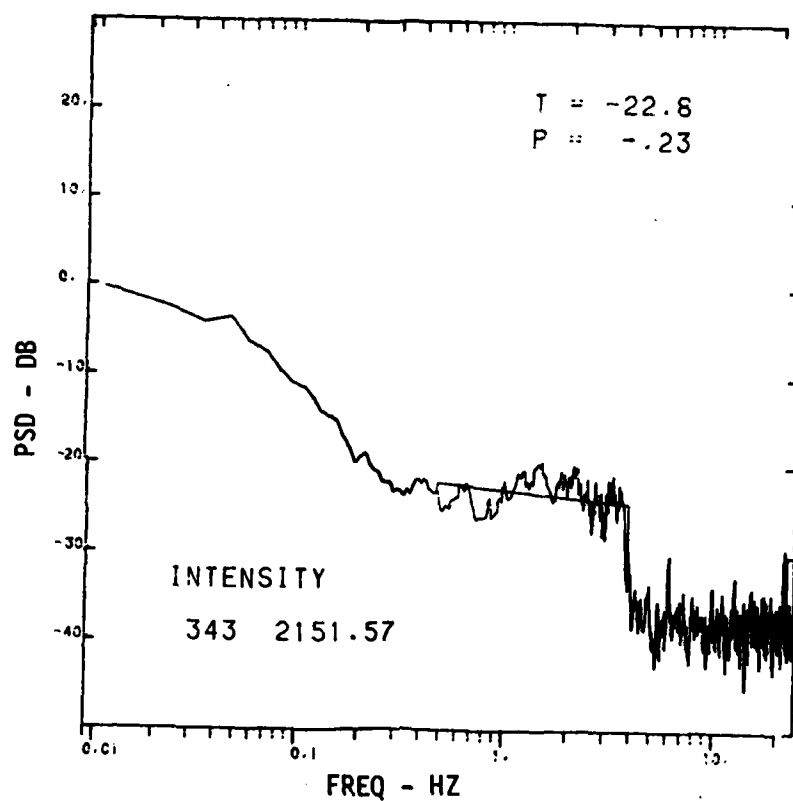


b) Pattern with Non-Zero Offset Frequency

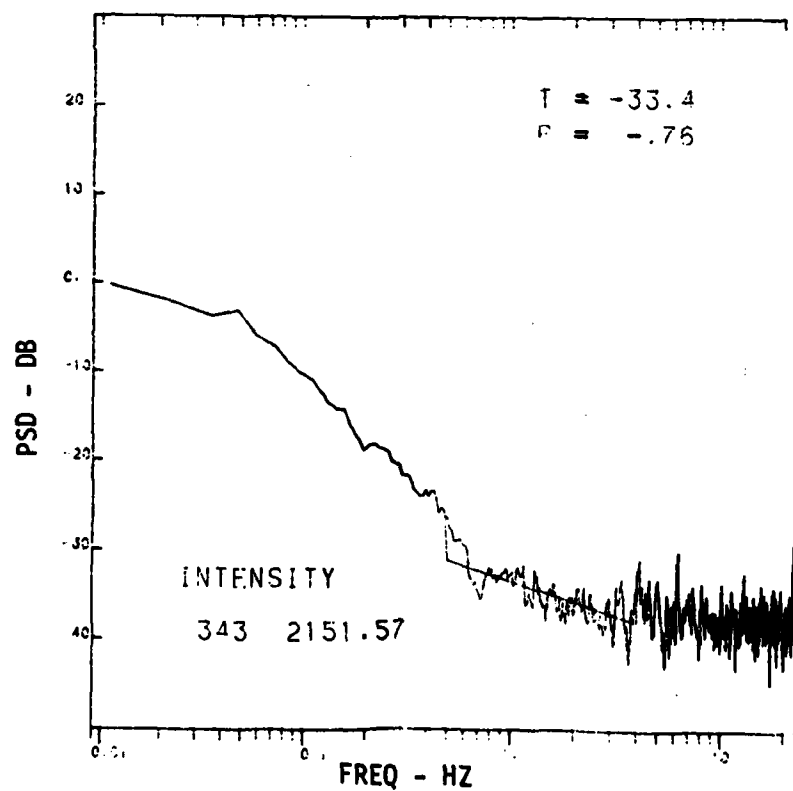


c) Case b) with Stable Leakage Signal Present

Figure 4. Sketches of Signal Scatter Plots Illustrating Effect of Offset Frequency and Coherent Leakage



a) Spectrum Before Cancellation of Leakage Signal



b) Spectrum After Cancellation of Leakage Signal

Figure 5. Illustration of Elimination of Coherent Leakage

Data analysts have an obligation to view with suspicion any process that involves modification of raw data and which, as a consequence, might affect the validity of their deductions.

Now, cancellation of coherent leakage is accomplished by adding to each of the quadrature components of the raw signal a quantity that is constant over the analysis period.

It is of interest to inquire how this procedure would affect the data if it were to function incorrectly. Consider two cases: data with coherent leakage present; and data that is free of leakage.

Leakage present. In this case the cancellation procedure, if it functions imperfectly, will either not fully suppress the leakage or it might actually increase the apparent level of leakage.

No leakage. In this case, the algorithm should estimate zero leakage and should not modify the data. If its estimate is in error, though, it will subtract this erroneous estimate from the data. The result will be data which will have the appearance of contamination by leakage.

Thus, a malfunction of the cure is manifested as symptoms of the disease. Analysts should monitor processed data for any such evidence.

2.4 References

- 1) Roberts, F.R., "Software for Processing Scintillation Data From Satellites in Eccentric Orbits," AFGL Technical Memorandum No. 81, April 7, 1983.

3.0 Program PROPLOK

3.1 Introduction

Ionospheric ducting and iono-to-iono mode propagation are familiar phenomena in the field of radio wave propagation. Their occurrence for ground-based stations, though, is generally dependent on the existence of special conditions such as suitably-oriented electron density gradients in the ionosphere. Thus, availability of ducted modes is dependent on the vagaries of the ionosphere. However, these modes offer some hope of affording coverage across regions throughout which the ionosphere is affected by disturbed conditions, precluding use of classical modes. There is interest, then, in providing man-made launching mechanisms (such as artificial field-aligned ionization) in order to make such modes available when needed. Satellite experiments are to be performed to explore this technology.

In the conduct of experiments, both classical and ducted modes will generally be observed. Each will exhibit both a characteristic "range" delay time and a Doppler frequency shift. A method of calculating Doppler shift and delay time will be required for both the planning of data collection and the analysis of measurements. Program PROPLOK has been developed to satisfy this requirement. PROPLOK is, basically, a variant of the satellite ephemeris program, LOKANGL, described in Reference 1.

Figure 1 illustrates the propagation geometry for both the ducted and classical modes. As presently configured, PROPLOK computes the range delay for the ducted modes exclusive of the launching up-leg which illuminates field-aligned ionization from which the ducted mode is scattered. For purposes of calculation, the ducted path is assumed to extend from the point directly above the station to the satellite location. The altitude of the path is assumed uniform and equal to the altitude of the satellite. Similarly, the reflection height for the classical mode(s) is assumed the same for each hop and is equal to the satellite altitude. PROPLOK performs calculations for the three lowest order modes capable of propagating, i.e., with elevation angle greater than some pre-set minimum value corresponding to the minimum radiation angle of the transmit antenna being used.

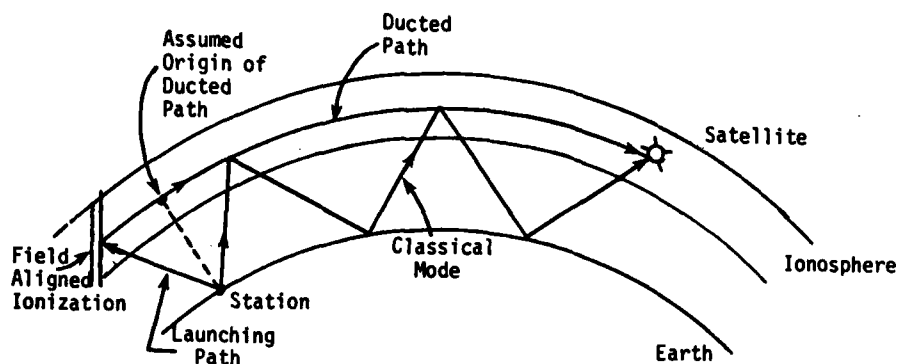


Figure 1. Propagation Geometry

3.2 Functional Description

PROPLOK is a modification of AFGL's standard satellite ephemeris program, LOKANGL, tailored to provide HF propagation calculations for ground station-to-satellite paths, taking account of the satellite's changing position and velocity as it traverses its orbit.

Major changes to LOKANGL are the following:

1. To reduce core requirements and permit use on INTERCOM, several unused subroutines are eliminated.
 - e.g., WRSTP, SOLVIL, SILL.
2. Input is totally revised.
 - Unchanging quantities are eliminated from the input process and written permanently into code.

- Element sets are input by means of a chronologically ordered permanent file. The latter is to be updated using NETED as new element sets are received.
 - User cues added.
 - Essentially, only analysis time-window is required as input (start date, time; stop date, time).
3. Propagation calculations are inserted in Subroutine SPPROU.
 4. Almost all standard LOKANGL output is suppressed, and new output is provided.

The basic LOKANGL package is used to furnish three types of data for propagation analysis:

1. Satellite coordinates (as function of time).
 - These, together with ground station locations, specify the propagation path geometry.
2. Satellite velocity components in station-centered spherical coordinate system (range, azimuth, elevation).
 - With vehicle velocity and ray path orientation at the satellite's location both expressed in the same coordinate frame, the Doppler shift of signals can be calculated.
3. Bearing of satellite from ground station.

In providing the foregoing ephemeris data, PROPLOK functions in the normal LOKANGL fashion, as described in Reference 1. Next, the ephemeris data is fed to the propagation calculations, the results of which are printed out. These functions are performed within subroutine SPPROU.

Figure 2 is a modified version of Figure 1 of Reference 1. Functions not performed in PROPLOK have been eliminated; new PROPLOK functions have been added to the drawing.

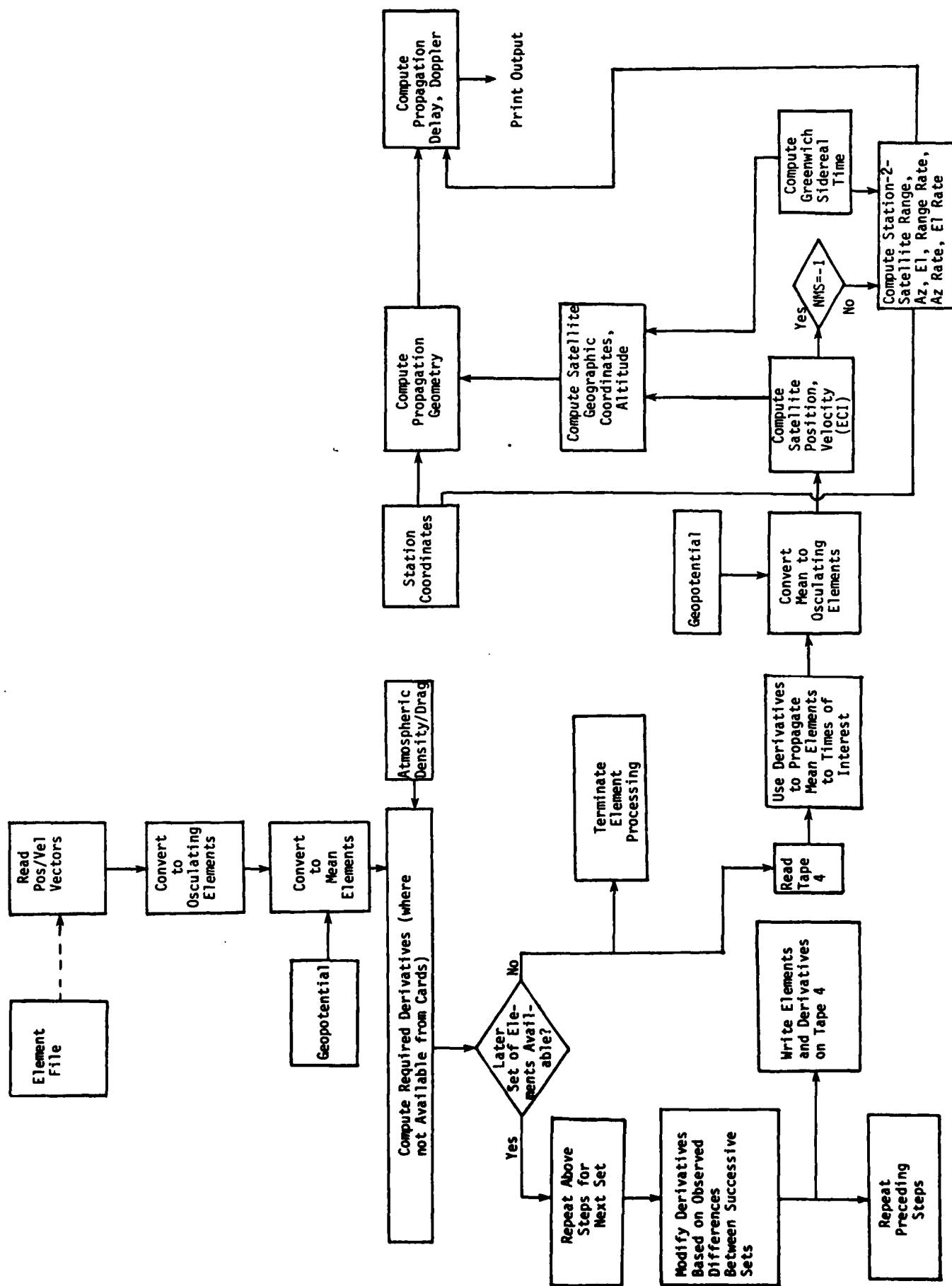


Figure 2. Simplified Operational and Data Flow for PROPLOK

The user is required to furnish minimal input data to PROPLOK consisting of:

- Time interval (seconds) between successive calculations
- Start time of run (year, month, day, hour, minute, second)
- End of time of run (year, month, day, hour, minute, second)

These data are inputted interactively in accordance with cues which are furnished.

Element sets for the satellite are obtained from a chronologically ordered file which must be attached for each run. PROPLOK scans this file and selects the appropriate elements.

3.3 Input and Output

The user is required to furnish minimal input data to PROPLOK consisting of:

- Time interval (seconds) between successive calculations
- Start time of run (year, month, day, hour, minute, second)
- End time of run (year, month, day, hour, minute, second)

These data are inputted interactively in accordance with cues which are furnished.

Element sets for the satellite are obtained from a chronologically ordered file, TAPE8 (ELSETFILE), which must be attached for each run. PROPLOK scans this file and selects the appropriate elements.

It is assumed that orbital data for the satellite which carries the instrumentation for the ducted mode experiments will be furnished as SCF

position/velocity vectors. records in the TAPE8 file consist of card images of these SCF cards, the format of which is given on page 62 of Reference 1.

An example of the output from PROPLOK is presented in Figure 3.

3.4 Mathematical Approach

3.4.1 Propagation Geometries

3.4.1.1 Classical Modes

The propagation geometry depends upon the coordinates of the ground station and the satellite. The former are fixed and are imbedded in the code. The latter are calculated in PROPLOK as described in Reference 1.

If

D = Total ground distance of path

and

C = Central angle subtended by total path

then

$$C = D/R = \arccos (\sin (LAT1) \sin (LAT2) + \cos (LAT1) \cos (LAT2) \cos (LON2 - LON1)) \quad (1)$$

where R = Radius of earth

$LAT1, LON1$ = Latitude and longitude of station

$LAT2, LON2$ = Latitude and longitude of satellite.

PREPARED BY/FOR THE ANALYSIS AND SIMULATION BRANCH (BUNY), AIR FORCE GEOPHYSICS LABORATORY, TELEPHONE 8414161

USER-PLEASE ENTER PRINT INTERVAL(SECONDS),START
AND STOP TIMES(MO,DA,YR,HR,MIN,SEC) IN THE FOLLOWING
FORMAT WITH EACH VALUE SEPARATED BY A COMMA.
F,I,I,I,F,F,F,I,I,I,F,F,F
F-FLOATING POINT,I-INTEGER, EXAMPLE BELOW.
300.,9,1,80,0.,0.,0.,9,1,80,2.,0.,0.
THIS WILL GIVE YOU 300 SECOND INTERVALS FROM 0-2 HRS
ON SEPT 1,1980
NOW MAKE YOUR ENTRY ON THE NEXT LINE, FOLLOWING
THE FORMAT AND ORDER OF THIS EXAMPLE

STATION DATA (NOTE-PROGRAM DEFINES NSG TO BE -2, HENCE LOOK ANGLES WILL BE MEASURED IN GEODETIC SYSTEM)

NUMBER	NAME	NSG	GEOD LAT. (DEG)	GEOD LAT. (DEG)	WEST LONG. (DEG)	ALTITUDE (KM)	RADIUS (KM)
1	AVA : : : : :	2	.43227933E+02	.43420000E+02	.75400000E+02	0.	.63681082E+04
2	K SALH: : : : :	2	.58228010E+02	.58400000E+02	.15640000E+03	0.	.63626897E+04

EPHEMERIS PRINTOUT DATA

	MONTH	DAY	YEAR	HR.	MIN.	SEC.
START PRINT TIME	8	1	78	0.	0.	0.000
END PRINT TIME	8	2	78	0.	0.	0.000

PRINT EVERY .36000000E+04(SECONDS)

										PROPAGATION TIME AND DERIV. OF PATH LENGTH (MILLISECONDS AND KM/SEC)									
										3 LOWEST ORDER CLASSICAL NODES									
ST	DATE						UT				SATELLITE LOCATION(DEG,KM)				DUCTED NODE				
NO	MO	DA	YR	HR	MIN	SEC	LAT	LONG	ALT	GD	RNG	DRG	H	T1	DP1	T2	DP2	T3	DP3
1	8	1	78	0	0	0.	82.77	84.71	190.11	4393.0	358.17		7	15.57	4.67	16.36	4.44	17.33	4.19
2	8	1	78	0	0	0.	82.77	84.71	190.11	3344.2	13.80		7	12.28	-5.87	13.24	-5.45	14.40	-5.02
1	8	1	78	1	0	0.	-29.95	35.02	265.08	9146.3	145.49		11	32.15	-6.91	32.81	-6.79	33.56	-6.65
2	8	1	78	1	0	0.	-29.95	35.02	265.08	14629.5	80.58		17	51.75	-6.25	52.41	-6.18	53.12	-6.11
1	8	1	78	2	0	0.	-34.20	238.01	221.40	18219.2	298.50		19	44.01	5.21	44.62	5.16	45.27	5.12
2	8	1	78	2	0	0.	-34.20	238.01	221.40	12752.2	244.10		15	45.05	6.51	45.71	6.43	46.44	6.35
1	8	1	78	3	0	0.	80.98	204.37	185.14	5856.7	351.17		9	20.93	7.33	21.71	7.07	22.63	6.79
2	8	1	78	3	0	0.	80.98	204.37	185.14	2931.9	344.78		5	10.24	2.10	11.03	1.95	12.08	1.78
1	8	1	78	4	0	0.	-20.32	81.33	257.29	7121.9	186.19		9	24.98	-7.17	25.66	-6.98	26.46	-6.78
2	8	1	78	4	0	0.	-20.32	81.33	257.29	11103.1	113.17		13	39.10	-6.71	39.75	-6.61	40.48	-6.51
1	8	1	78	5	0	0.	-43.93	284.82	233.00	17680.6	101.61		19	62.26	.34	62.88	.34	63.54	.33
2	8	1	78	5	0	0.	-43.93	284.82	233.00	16211.4	271.80		17	56.89	5.69	57.50	5.64	58.15	5.58
1	8	1	78	6	0	0.	72.41	273.21	180.72	7068.9	5.93		9	24.81	5.99	25.50	5.83	26.30	5.66
2	8	1	78	6	0	0.	72.41	273.21	180.72	4701.1	336.34		7	16.55	6.91	17.30	6.62	18.23	6.30

Figure 3. Sample Output From PROPLOK

Since arc cos returns an angle in the range (0, 180°), we are assured that the results apply to the "short" path. We assume:

- the propagation path is comprised of N half-hops, where N is always an odd integer.
- ionospheric reflection heights along the path and satellite altitude are all equal and are denoted H.

Examining the geometry of Figure 4, we observe that, for right-triangle QAB:

$$P = R \sin (C/N) / \cos (E + C/N). \quad (2)$$

Here

P = Propagation path length of single half-hop

C = Central angle of total path

C/N = Central angle of a half-hop

R = Radius of earth

H = Height of ionosphere.

Referring again to Figure 4, we can also write

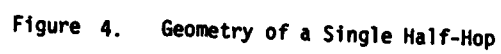
$$P \sin(E + C/N) = H + R(1 - \cos(C/N)) \quad (3)$$

where E is the elevation angle of the radio wave. Eliminating P from (2) and (3), we have:

$$E = \arctan((H + R(1 - \cos(C/N))) / R \sin(C/N)) - C/N. \quad (4)$$

Knowing the coordinates of both the station and the satellite, we can use these relations to solve for the key propagation parameters, E and P, for the classical modes.

The PROPLOK calculation begins by assuming N = 1 (where N is the number of half hops) and calculates E. N is then incremented by 2 and the solution repeated. The process repeats until E is equal to or greater than a



specified minimum value, which typically could be zero or the minimum effective take-off angle for the particular antenna used at the station. We have now identified the lowest order propagating mode. N is then incremented twice more to provide calculations for each of the three lowest order propagating modes.

3.4.1.2 Ducted Mode

The propagation path for the ducted mode is taken to be a circular arc, concentric with the earth, at the uniform ionospheric height H. This is illustrated in Figure 5. This arc extends from the point directly above the station to the satellite. The propagation path is given by:

$$P_D = (R + H) \cdot C \quad .$$

3.4.2. Propagation Range Rate

The Doppler frequency shift imparted by motion of the satellite is obtained from the time derivative of propagation range. This quantity is determined from the scalar product of vehicle velocity and the unit vector at the satellite location aligned in the direction of propagation. LOKANGL provides vehicle velocity expressed in terms of station look angle coordinates: time rates of change of (station) range, azimuth, and elevation. The azimuthal component of vehicle velocity is transverse to the plane of propagation and, therefore, makes no contribution. The propagation range rate is found, then, by combining the contributions of the range and elevation components.

3.4.2.1 Classical Modes

The geometry for propagation range rate calculation is shown in Figure 6. The calculation requires the value of angle B. Observe that angle D is given by:

$$D = 90^\circ - C - EL$$

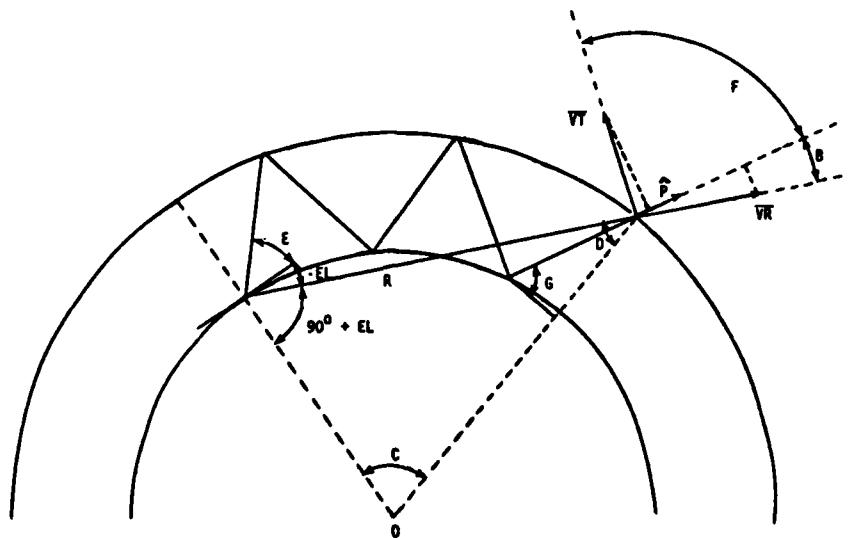


Figure 6. Geometry for Range Rate Calculation for Classical Modes

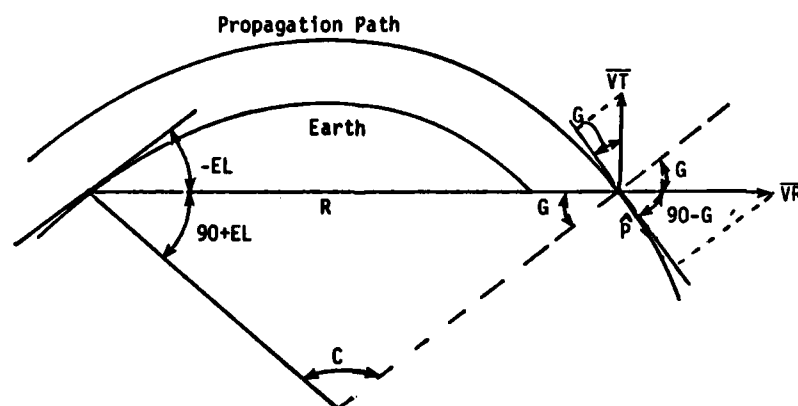


Figure 7. Geometry for Range Rate Calculation for the Ducted Mode

where EL is the elevation look angle. Now

$$B = D - (90 - G) \quad .$$

From Figure 4 showing the half-hop geometry, it may be observed that

$$G = E + C/N \quad .$$

Therefore

$$B = E - EL - C (1 - 1/N) \quad .$$

The radial component of velocity makes the contribution

$$VR \cos B \quad ,$$

and the elevation contribution is

$$VT \sin B \quad .$$

3.4.2.2 Ducted Mode

The geometry for this case is shown in Figure 7. The radial component makes the contribution

$$VR \cos (90^\circ - G) = VR \sin G \quad ,$$

and the elevation contribution is

$$- VT \cos G \quad .$$

The range rate is given by their sum.

3.5 References

- 1) Bass, J.N., et al, "Analysis and Programming for Research in the Physics of the Upper Atmosphere," AFGL-TR-81-0293, Logicon Final Report, October 9, 1981.